

# Reactions of $P_4$ and $I_2$ with $Ag[Al(OC(CF_3)_3)_4]$ : from elusive polyphosphorus cations to subvalent $P_3I_6^+$ and phosphorus rich $P_5I_2^+$ †

Ingo Krossing

University of Karlsruhe, Engesserstr. Geb. 30.45, 76128 Karlsruhe, Germany.  
 E-mail: krossing@chemie.uni-karlsruhe.de

Received 3rd May 2001, Accepted 5th November 2001

First published as an Advance Article on the web 29th January 2002

Reactions of  $X_2$  ( $X = Br, I$ ),  $P_4$  and  $Ag(CH_2Cl_2)[Al(OR)_4]$  [ $R = C(CF_3)_3$ ] in suitable ratios to prepare naked polyphosphorus cations were carried out and led to products which suggested the presence of these elusive cations as intermediates. At temperatures above  $-30\text{ }^\circ\text{C}$  to rt the initially formed cations decomposed the  $Al(OR)_4^-$  anion giving, in two cases, the more stable fluoride bridged  $(RO)_3Al-F-Al(OR)_3^-$  anion. When  $Br_2$  was used as the oxidising agent the proposed intermediate phosphorus cation ( $P_5^{+?}$ ) reacted with the solvent  $CDCl_3$  by double insertion of a  $P^+$  unit into the C–Cl bond giving  $Cl_2P(CDCl_2)_2[(RO)_3Al-F-Al(OR)_3]$ , **1**. When  $I_2$  was used as the oxidiser the reaction led to the marginally stable  $P_3I_6[(RO)_3Al-F-Al(OR)_3]$ , **2** (X-ray). By using very mild conditions throughout ( $-80\text{ }^\circ\text{C}$ ) the primary product of the reaction of  $Ag(P_4)_2[Al(OR)_4]$  and  $I_2$  was isolated:  $P_5I_2[Al(OR)_4]$ , **3**, containing the  $P_5I_2^+$  cation with a hitherto unknown  $C_{2v}$ -symmetric  $P_5$  cage as structural building block.  $P_3I_6[Al(OR)_4]$ , **4**, was directly synthesised in quantitative yield starting from  $P_2I_4$ ,  $PI_3$  and  $Ag(CH_2Cl_2)[Al(OR)_4]$  in  $CH_2Cl_2$  solution.  $P_3I_6^+$  is formed through the  $P_2I_5^+$  stage ( $^{31}\text{P-NMR}$ ).  $P_3I_6^+$  (av.:  $P^{2.33}$ ) is the first subvalent P–X cation ( $X = H, F, Cl, Br, I$ ).  $P_5I_2^+$  (av.:  $P^{0.6}$ ) is the first phosphorus rich binary P–X cation. They are the third and fourth example of a binary P–X cation after the known  $PX_4^+$  and  $P_2X_5^+$  cations. The observed reactions were fully accounted for by thermochemical Born–Haber cycles based on (RI)-MP2/TZVPP *ab initio*, COSMO solvation and lattice enthalpy calculations (all phases). The gaseous enthalpies of formation of several species were calculated to be (in  $\text{kJ mol}^{-1}$ ):  $P_5^+$  (913),  $P_3I_6^+$  (694),  $P_5I_2^+$  (792),  $P_2I_5^+$  (733),  $Ag(P_4)_2^+$  (784).

## Introduction

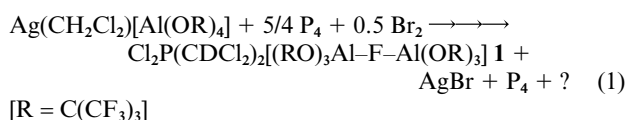
Phosphorus, arsenic and fluorine are the only electronegative non-metallic elements for which homopolyatomic elemental cations are still unknown as “compounds in the bottle”. For P and As this appears rare, since gaseous phosphorus and arsenic cations are well investigated by mass spectrometric measurements (up to  $P_{89}^+$ ),<sup>1,2</sup> photo ionisation studies ( $E_{2-5}^+$ ,  $E = P, As$ )<sup>3</sup> and theoretical investigations.<sup>1c,4</sup> Many of the basic thermodynamic properties of  $E_n^+$  (*i.e.*  $IP^+$ s,  $\Delta_rH$ ) are known.<sup>5</sup> (Radical-) Cations  $E_n^+$  with an even number,  $n$ , of elemental atoms were shown to be considerably less stable than the diamagnetic uneven species  $E_n^+$ .<sup>4</sup> However, earlier work showed that classical approaches to salts of  $E_n^+$  (*i.e.* oxidation of E by  $MF_5$  or  $F_2S_2O_6$ ,  $M = As, Sb$ ) did not lead to success but rather to a decomposition of the anions and formation of E–O and E–F species.<sup>6</sup> And, indeed, the strengths of the E–F bonds (484 and  $490\text{ kJ mol}^{-1}$  in  $EF_3$ )<sup>5</sup> are amongst the highest known in the periodic table and therefore account for the decomposition reactions. To circumvent the decomposition of the anions, we employed a new generation of weakly basic anions of type  $Al(OR)_4^-$  [ $R = C(CF_3)_3$ ], the syntheses of lithium and silver salts of which was recently published by Strauss<sup>7</sup> and us.<sup>8</sup>  $Al[OC(CF_3)_3]_4^-$  also appeared to be an ideal spectator ion, since it stabilises the unusual  $D_{2h}$  symmetric homoleptic  $Ag(P_4)_2^+$  cation.<sup>9</sup> Previously we showed<sup>8</sup> that the  $Al[OC(CF_3)_3]_4^-$  anion, which is stable in 35%  $HNO_3$ , is one of the most weakly coordinating anions known. Herein we present the results of our efforts to oxidise the silver- $P_4$  adducts<sup>9</sup> with halogens

that finally led to the formation of salts of the  $P_3I_6^+$  and  $P_5I_2^+$  cations. A preliminary account on  $P_5I_2^+$  has been given.<sup>10</sup>

## Results

### Syntheses and spectroscopic characterisation

Initial reactions of  $Li[Al(OR)_4]$ ,  $P_4$  and iodine [ $R = C(CF_3)_3$ ] in various solvents in suitable ratios for the preparation of  $P_5^+$  only led to an orange–red solid material, which, according to the Raman spectra, did not contain the anion but rather was a mixture of red phosphorus and  $P_2I_4$ . This was attributed to the very hard and polarising  $Li^+$  cation that, with the reaction conditions employed, didn't react with the soft phosphorus iodides. However, when exchanging  $Li^+$  for  $Ag^+$  and  $I_2$  for  $Br_2$  an ionisation occurred as shown by the NMR scale reaction of  $Ag(CH_2Cl_2)[Al(OR)_4]$ ,  $5/4 P_4$  and  $0.5 Br_2$  in  $CDCl_3$  [see eqn. (1)]:

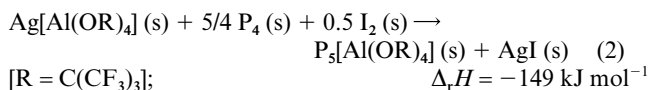


The unit cell of several of the uniform colourless crystals of this reaction was determined and all of them showed the same triclinic cell as **1** indicating that this was the main product of reaction (apart from  $P_4$ ). The rt  $^{31}\text{P-NMR}$  of this solution showed two lines: an intense line attributable to  $P_4$  and another weaker resonance we assign to the  $Cl_2P(CDCl_2)_2^+$  cation (144 ppm, *cf.* 96 ppm in  $PCl_4^+PCl_6^-$ ). Presumably a very electrophilic phosphorus cation [*e.g.*  $P_5^+$ , *cf.* eqn. (2)] was initially formed

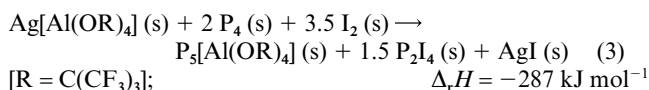
† Electronic supplementary information (ESI) available: a drawing of the single piece apparatus used for the reactions. See <http://www.rsc.org/suppdata/dt/b1/b103957c/>

which decomposed the anion and finally led to the observed products. The formation of the  $\text{Cl}_2\text{P}(\text{CDCl}_2)_2^+$  cation in **1** is then seen as a double insertion of a  $\text{P}^+$  unit (possibly from  $\text{P}_5^+$ ) into a C–Cl bond (see Discussion).

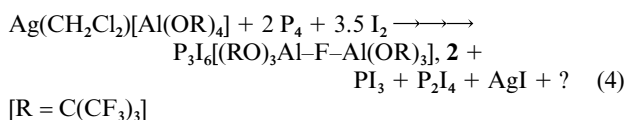
We concluded that iodine should be a more suitable oxidising agent than bromine since it is solid and reactions are, therefore, slower. A thermochemical evaluation<sup>11,12</sup> of eqn. (2) showed it to be favourable by  $149 \text{ kJ mol}^{-1}$ :



More polar solvents such as  $\text{CH}_2\text{Cl}_2$  (*cf.*  $\epsilon = 8.9$  vs. 4.8 for  $\text{CHCl}_3$ )<sup>5c</sup> should also help to stabilise the ions (*cf.* the computational work below). Therefore a reaction as in eqn. (2) was performed in  $\text{CH}_2\text{Cl}_2$ . The reaction temperature in this experiment was always kept below  $-20^\circ\text{C}$  and immediately after consumption of all visible amounts of iodine part of the orange coloured solution was poured into a glass tube. All volatiles were then removed *in vacuo* and the Raman spectrum of the remaining orange material showed bands attributable to the intact anion,  $\text{Ag}(\text{P}_4)_2^+$ ,  $\text{P}_2\text{I}_4$  but also new P–P stretches that possibly stem from yet unknown phosphorus cations  $\text{P}_n^+$  ( $n = 3, 5, 7$ ).<sup>13</sup> In further reactions according to eqn. (2) the presence of larger amounts of  $\text{P}_2\text{I}_4$  was reinforced by the isolation of orange triclinic crystals which, according to their unit cell<sup>14</sup> and Raman spectrum, were  $\text{P}_2\text{I}_4$ . Therefore  $\text{P}_2\text{I}_4$  appeared to be a thermodynamic sink in this reaction. To exploit the formation of  $\text{P}_2\text{I}_4$  as an additional driving force the underlying thermochemistry<sup>11</sup> was examined in a suitable cycle [see eqn. (3)].



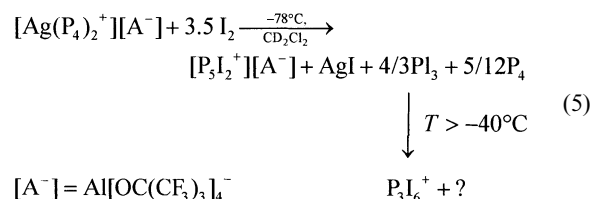
Indeed we found that eqn. (3) should be considerably more favourable than a reaction according to eqn. (2)  $\{\Delta_r H [\text{eqn. (3)}] = -287 \text{ kJ mol}^{-1}$  vs.  $\Delta_r H [\text{eqn. (2)}] = -149 \text{ kJ mol}^{-1}\}$ . Consequently eqn. (3) was initially performed in  $\text{CH}_2\text{Cl}_2$  and after stirring the reaction mixture overnight at  $-30^\circ\text{C}$  all volatiles were removed. To extract the very  $\text{CS}_2$  soluble by-product,  $\text{P}_2\text{I}_4$ , the solid yellow–orange residue was extracted with  $\text{CS}_2$  at *rt*<sup>15</sup> and, to our surprise, much of the solid material was soluble in this very non-polar solvent. From the concentrated  $\text{CS}_2$  solution of this reaction we obtained a mixture of single crystals. Amongst orange  $\text{P}_2\text{I}_4$  needles (unit cell determination<sup>14</sup> and Raman) a larger amount of yellow plate-like and extremely sensitive crystals was found and the single crystal X-ray structure determination of these yellow plates showed them to be  $\text{P}_3\text{I}_6[(\text{RO})_3\text{Al–F–Al}(\text{OR})_3]$ , **2**, containing the first subvalent binary P–X cation ( $\text{X} = \text{H, F, Cl, Br, I}$ ) with an average oxidation state of P of 2.33. In the  $^{31}\text{P}$ -NMR of this  $\text{CS}_2$  solution lines attributable to  $\text{PI}_3$  and  $\text{P}_2\text{I}_4$  appeared at  $\delta^{31}\text{P} = 176$  and 105 but were very broad ( $\nu_{1/2} = 2100$  and 1600 Hz) indicating rapid exchange (with  $\text{P}_3\text{I}_6^+$ ). Repeating the  $^{31}\text{P}$ -NMR spectra at low temperature ( $-30$  and  $-70^\circ\text{C}$ ) led to sharp lines ( $\nu_{1/2} = 5$  Hz) with greatly enhanced signal-to-noise ratio at the expected positions for  $\text{PI}_3$  and  $\text{P}_2\text{I}_4$  at  $\delta^{31}\text{P}(-30^\circ\text{C}$  and  $-70^\circ\text{C}) = 176$  and 105, but no additional lines due to a P-containing cation emerged—indicating that the cation had precipitated or that a fast exchange between the unknown species ( $\text{P}_3\text{I}_6^+$ ) and  $\text{PI}_3$ ,  $\text{P}_2\text{I}_4$  or the solvent was still occurring. The overall reaction with all observed products is given in eqn. (4):



The obtained  $\text{P}_3\text{I}_6^+$  salt was always contaminated with the very intense Raman scatterer  $\text{P}_2\text{I}_4$  which prevented its Raman observation, however, we succeeded in the independent direct synthesis of  $\text{P}_3\text{I}_6^+$  (see below).

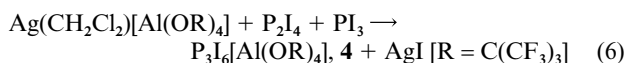
We reinvestigated the reaction as proposed in eqn. (3) by low temperature *in situ* NMR spectroscopy but using pure  $[\text{Ag}(\text{P}_4)_2][\text{Al}(\text{OR})_4]^9$  instead of the  $\text{Ag}(\text{CH}_2\text{Cl}_2)[\text{Al}(\text{OR})_4]/2 \text{P}_4$  mixture. When  $[\text{Ag}(\text{P}_4)_2][\text{Al}(\text{OR})_4]^9$  in  $\text{CD}_2\text{Cl}_2$  was reacted with 3.5 equivalents of  $\text{I}_2$  at  $-78^\circ\text{C}$  one major product was observed in the *in situ*  $^{31}\text{P}$ -NMR spectrum ( $-90^\circ\text{C}$ ) recorded after 30 minutes:  $[\text{P}_5\text{I}_2][\text{Al}(\text{OR})_4]$  **3** [eqn. (5)] containing a  $\text{C}_{2v}$ -symmetric  $\text{P}_5\text{I}_2^+$  cation, the *in situ*  $^{31}\text{P}$ -NMR spectrum of which is shown in Fig. 1.

Both pure  $\text{PI}_3$  and  $\text{P}_2\text{I}_4$  are insoluble in  $\text{CD}_2\text{Cl}_2$  at these temperatures ( $^{31}\text{P}$ -NMR) and, therefore, exchange with the cation as in  $\text{CS}_2$  did not occur. Small amounts of solid  $\text{P}_4$  were also visible in the  $^{31}\text{P}$ -NMR (not shown).<sup>16</sup> A larger preparative reaction, always kept at  $-80^\circ\text{C}$ , verified these conclusions based on the mass balance, the Raman observation of pure  $\text{P}_5\text{I}_2^+[\text{Al}(\text{OR})_4]$  **3** in the soluble and  $\text{PI}_3$ ,  $\text{P}_4$  and traces of  $\text{P}_2\text{I}_4$  in the insoluble material of this reaction as well as an elemental analysis of **3**. The balanced overall reaction with the observed products is given in eqn. (5):



Solid pure **3** may be handled at *rt* for 1–2 hours, however, upon warming the NMR tube overnight to  $-40^\circ\text{C}$  the  $\text{P}_5\text{I}_2^+$  signals vanish and, apart from other unassigned signals of lower intensity, those of  $\text{P}_3\text{I}_6^+$  appear as major P-containing peaks (*cf.*  $\text{P}_3\text{I}_6^+[\text{Al}(\text{OR})_4]$ , **4**, below). The observation of only traces of  $\text{P}_2\text{I}_4$  but large amounts of  $\text{PI}_3$  in the Raman spectrum, at  $-80^\circ\text{C}$ , of the insoluble material of eqn. (5) shows that in the earlier reactions  $\text{P}_2\text{I}_4$ , which was always found, is formed from  $\text{PI}_3$  and  $\text{P}_4$  only upon warming. Initial  $\text{PI}_3$  formation is in agreement with Tattershall's<sup>17</sup> earlier observation that  $\text{P}_4$  reacts with  $\text{I}_2$  to immediately give  $\text{PI}_3$  which is then reduced by  $\text{P}_4$  giving  $\text{P}_2\text{I}_4$ . From the Raman spectrum<sup>18</sup> of the very air and moisture sensitive solid yellow **3**, shown in Fig. 2, the presence of the intact  $\text{Al}(\text{OR})_4^-$  anion  $\{796$  and  $745 \text{ cm}^{-1}$ , *cf.*  $798$  and  $746 \text{ cm}^{-1}$  in  $\text{Ag}(\text{P}_4)_2[\text{Al}(\text{OR})_4]^9\}$  as well as a P–I stretch at  $168 \text{ cm}^{-1}$  immediately follow and support the assignment of the  $\text{P}_5\text{I}_2^+$  cation (see Discussion).

With the awareness of the  $\text{P}_3\text{I}_6^+$  cation we succeeded in directly synthesising this species by reacting  $\text{PI}_3$ ,  $\text{P}_2\text{I}_4$  and  $\text{Ag}(\text{CH}_2\text{Cl}_2)[\text{Al}(\text{OR})_4]$  according to eqn. (6).



After 12 h at  $-78^\circ\text{C}$  the obtained yellow–orange solution (over an  $\text{AgI}$  precipitate) was investigated by variable temperature  $^{31}\text{P}$ -NMR spectroscopy, shown in Fig. 3.

Only at very low temperatures (below  $-80^\circ\text{C}$ ) was the resolution of the spectra good enough to resolve P–P coupling.  $\text{P}_3\text{I}_6^+$  was identified as main product (62% P), smaller amounts of  $\text{P}_2\text{I}_5^+$  were also visible (28% P).<sup>19</sup> After two weeks storage at  $-30^\circ\text{C}$  the  $\text{P}_2\text{I}_5^+$  was no longer visible in the  $-90^\circ\text{C}$   $^{31}\text{P}$ -NMR spectrum leaving  $\text{P}_3\text{I}_6^+$  as the only observed P-containing species. This suggests that the formation of  $\text{P}_3\text{I}_6^+$  proceeds through  $\text{P}_2\text{I}_5^+$ . The formation of **4** as the only remaining P-containing species according to eqn. (6) was verified in solution ( $^{31}\text{P}$ -NMR) and solid state (elemental analysis) on a larger

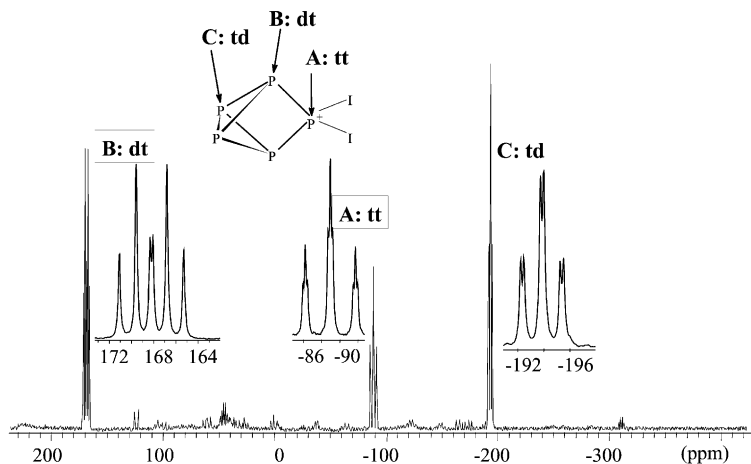


Fig. 1 *In situ*  $^{31}\text{P}$ -NMR spectrum of  $\text{P}_5\text{I}_2^+$  in **3** at  $-90^\circ\text{C}$ . td = triplet of doublets, dt = doublet of triplets, tt = triplet of triplets.

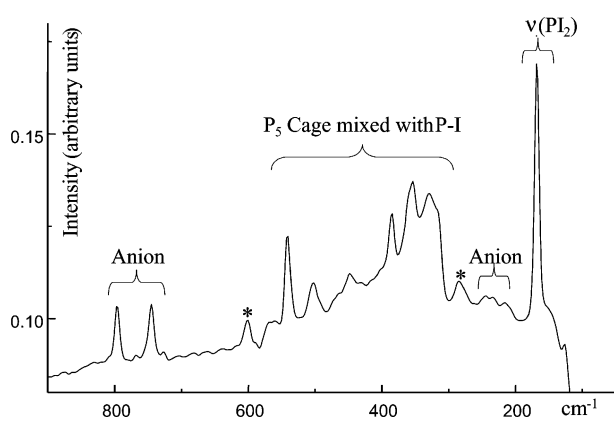


Fig. 2 Raman spectrum of solid **3**. Bands marked with an asterisk show small impurities due to the 100%  $A_1$  breathing modes of the very intense Raman scatterers  $\text{P}_4$  ( $600\text{ cm}^{-1}$ ) and  $\text{PI}_3$  ( $284\text{ cm}^{-1}$ ).<sup>18</sup>

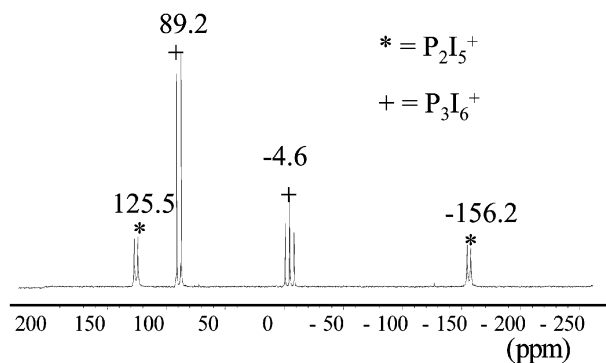


Fig. 3 NMR spectrum of the reaction of  $1.0\text{ P}_2\text{I}_4 + 1.0\text{ PI}_3 + 1.0\text{ Ag}[\text{Al}(\text{OR})_4]$  after 12 h at  $-78^\circ\text{C}$  in  $\text{CD}_2\text{Cl}_2$  at  $-90^\circ\text{C}$ .

preparative scale, however, we were unable to grow single crystals of **4**. Concentrated crystallisation samples always disproportionated giving  $\text{P}_2\text{I}_4$  and  $\text{P}_2\text{I}_5[\text{Al}(\text{OR})_4]^{20}$  (Raman, unit cell determination). Raman samples prepared from the yellow solid obtained upon removal of all volatiles from the orange-yellow  $\text{CH}_2\text{Cl}_2$  solution of **4** decomposed rapidly in the beam of the laser ( $1064\text{ nm}$ ) even with wide focus and low laser energy. In  $\text{CD}_2\text{Cl}_2$  solution the approximately  $C_2$  symmetric  $\text{P}_3\text{I}_6^+$  cation (see X-ray) gave the expected doublet ( $\delta^{31}\text{P} = 89.2$ ,  $^1J_{\text{pp}} = 385.5\text{ Hz}$ ) and triplet ( $\delta^{31}\text{P} = -4.6$ ,  $^1J_{\text{pp}} = 385.5\text{ Hz}$ ) with a 2 : 1 intensity ratio while the approximately  $C_s$  symmetric  $\text{P}_2\text{I}_5^+$  cation<sup>21</sup> gave two doublets at  $\delta^{31}\text{P} = 127.4$  and  $-156.3$  with a

coupling constant of  $^1J_{\text{pp}} = 320.2\text{ Hz}$  (1 : 1 intensity ratio). In contrast, the  $\text{P}_2\text{I}_5^+$  cation in  $\text{P}_2\text{I}_5\text{AlI}_4$  is only stable in the solid state and NMR spectra of  $\text{CS}_2$  solutions of the salt showed the signals of  $\text{PI}_3$  and  $\text{AlI}_3$ .<sup>22</sup> The solid state  $^{31}\text{P}$ -MAS-NMR spectrum of  $\text{P}_2\text{I}_5\text{AlI}_4$ <sup>22</sup> showed two broad resonances centred at  $\delta^{31}\text{P} = +114$  and  $-142$ ,<sup>22</sup> confirming the assignment of our solution values.<sup>20</sup>

To determine the activation energy for the exchange between the two different P atoms in  $\text{P}_3\text{I}_6^+$  the coalescence temperature was determined by a series of spectra ran at temperatures between 183 and 298 K (see Fig. 4). Using the Eyring-

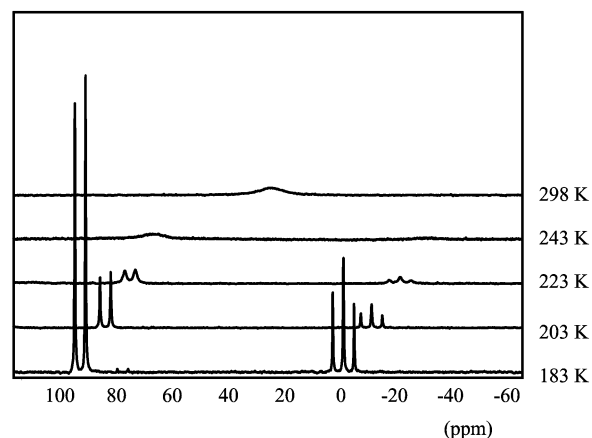


Fig. 4 Spectra of  $\text{P}_3\text{I}_6^+$  between 183 and 298 K; coalescence of  $\text{P}_3\text{I}_6^+$  at 243 K.

equation<sup>23</sup> and the coalescence temperature of 243 K the free energy of activation for the exchange of the two different phosphorus nuclei A and B in  $\text{I}_2\text{P}^{\text{A}}-\text{P}^{\text{B}}\text{I}_2-\text{P}^{\text{A}}\text{I}_2^+$  ( $= \text{P}_3\text{I}_6^+$ ) was estimated as:

$$\Delta G^\ddagger(\text{P}^{\text{A}} \rightarrow \text{P}^{\text{B}}) = 38.9\text{ kJ mol}^{-1}$$

### Crystal structures

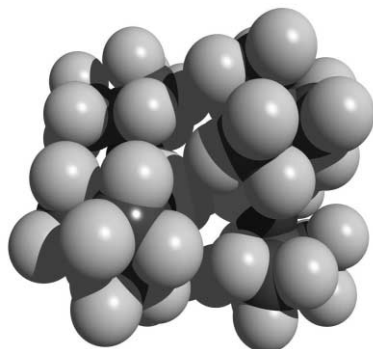
Details on the crystal structure solution and refinement are included in Table 6 (see Experimental).

**The  $\text{Cl}_2\text{P}(\text{CDCl}_2)_2^+$  cation in **1**.** Colourless block-like triclinic crystals of **1** (space group  $P\bar{1}$ ) grew in a sealed NMR tube of a NMR-scale reaction. Although the quality of the structure is not very good,<sup>24</sup> the cation—in contrast to the  $\text{CF}_3$  groups of the anion—is well behaved with reasonable standard deviations and shall therefore be briefly described (Fig. 5).  $\text{Cl}_2\text{P}(\text{CDCl}_2)_2^+$  may be derived from  $\text{PCl}_4^+$  by replacing two Cl atoms by



**Table 1** Comparison of the structural parameters of the  $(\text{RO})_3\text{Al-F-Al}(\text{OR})_3^-$  anions in **1**, **2** and the  $\text{Al}(\text{OR})_4^-$  anion [ $\text{Ag}(\text{Cl}_2\text{C}_2\text{H}_4)_3^+$  salt]

Parameter	<b>1</b>	<b>2</b>	$\text{Al}(\text{OR})_4^-$
$d(\text{Al-O})$ range/Å	1.681(4)–1.719(5)	1.671(9)–1.700(9)	1.714(3)–1.736(3)
$d(\text{Al-O})_{\text{av}}$ /Å	1.692	1.687	1.725
$(\text{Al-O-C})_{\text{av}}/^\circ$	152.8	154.9	149.5
$d(\text{Al-F})$ range/Å	1.761(3)–1.761(3)	1.760(4)–1.761(4)	—
$d(\text{Al-F})_{\text{av}}$ /Å	1.761	1.761	—
$(\text{Al-F-Al})/^\circ$	176.6(2)	180	—

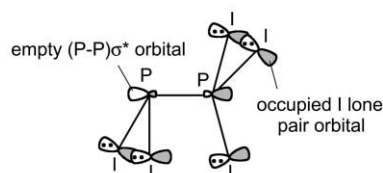
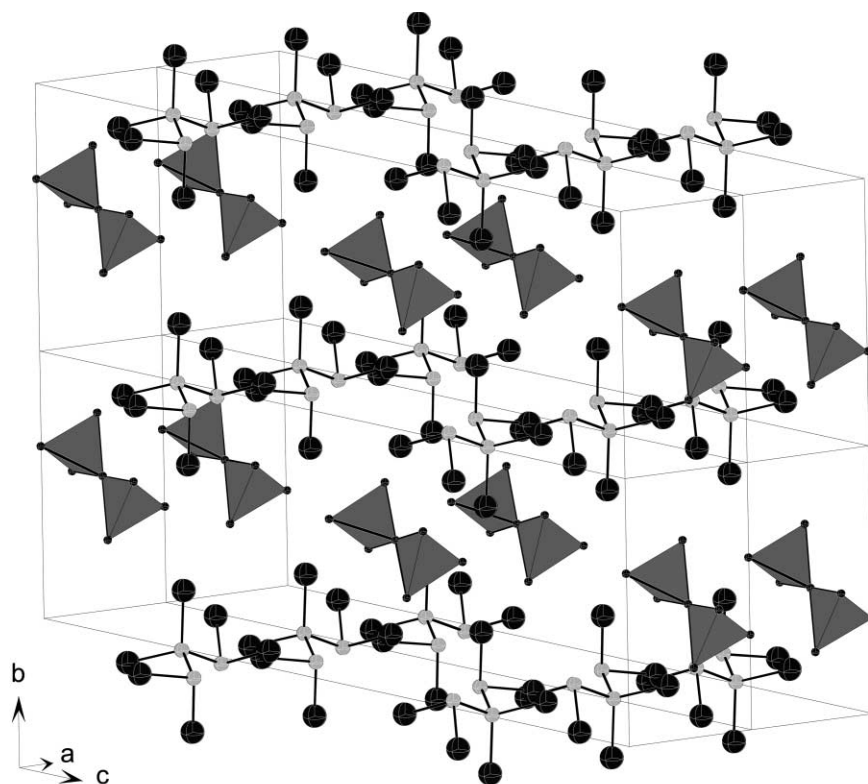
**Fig. 8** Space filling representation of the  $(\text{RO})_3\text{Al-F-Al}(\text{OR})_3^-$  anion.

as opposed to the homopolyatomic phosphorus cations, we fully optimised the geometries of  $\text{P}_3\text{I}_6^+$  ( $C_2$ ),  $\text{P}_5\text{I}_2^+$  ( $C_{2v}$ ),  $\text{P}_2\text{I}_5^+$  ( $C_s$ ),  $\text{P}_2\text{I}_4$  ( $C_{2h}$ ),  $\text{PI}_3$  ( $C_s$ ),  $\text{P}_5^+$  ( $C_{4v}$ ),  $\text{P}_4$  ( $T_d$ ),  $\text{Ag}(\text{P}_4)_2^+$  ( $D_{2h}$ ),  $\text{I}_2$  ( $D_{6h}$ ) and  $\text{AgI}$  ( $C_1$ ) at the BP86/SVP, B3LYP/TZVPP and MP2/TZVPP levels. A careful analysis of the computed structural parameters revealed that both pure DFT (BP86) and hybrid HF-DFT (B3LYP) were not capable of reproducing the structural parameters of the experimental geometries. The newer DFT MPWPW91 and, to a lesser extent, the HF-DFT MPW1PW91 levels also failed to give satisfactory geometries. However, at the (RI-)MP2/TZVPP level geometries with structural parameters close to the experimental data were obtained. This may be exemplified by a comparison of the

computed and experimental geometries of the  $\text{P}_2\text{I}_5^+$  and  $\text{P}_3\text{I}_6^+$  cations in Table 2.

Table 2 shows that the length of the P–P bond is sensitive to the level of theory chosen and therefore is a good indicator for the quality of the computation. The longest P–P bonds were obtained by BP86/SVP (0.14 to 0.17 Å too long). Only MP2 (and to a lesser extent MPW1PW91) gave acceptable P–P distances that were about 0.03 Å too long. A reason for this discrepancy may be found in the possible interaction of the occupied lone pair orbitals at the iodine atoms [= LP(I)] with the empty  $(\text{P-P})\sigma^*$  orbital [=  $\sigma^*(\text{P-P})$ ] as shown for  $\text{P}_2\text{I}_5^+$  in Fig. 10.

This electron transfer from LP(I)  $\rightarrow$   $\sigma^*(\text{P-P})$  should considerably elongate the P–P bond but only slightly shorten the P–I bonds. With the basis sets employed DFT and HF-DFT theory appeared to overestimate the interaction, as shown in Fig. 10, and therefore gave very long P–P bonds. Consequently only the structural parameters of the species computed with MP2 were collected in Fig. 11.

**Fig. 10** Possible interaction leading to elongation of the P–P bond in the DFT and HF-DFT optimisations.**Fig. 9** Solid state packing of **2**. All carbon and fluorine atoms (apart from those in the Al–F–Al linkages) are omitted for clarity. The  $\text{F}(\text{AlO}_3)_2$  units are shown as polyhedra and the cations as ball and stick representations (P: light grey, I: dark grey).

**Table 2** Comparison of the computed and experimental geometries of the  $P_2I_5^+$  and  $P_3I_6^+$  cations. Distances are given in Å

	Exp. <sub>(av.)</sub> <sup>a</sup>	MP2 <sup>b</sup>	BP86 <sup>c</sup>	B3LYP <sup>b</sup>	MPWPW91 <sup>d</sup>	MPW1PW91 <sup>d</sup>
<b><math>P_3I_6^+</math></b>						
P–P	2.213	2.247	2.355	2.328	2.315	2.270
$I_2P^+(PI_2)_2$	2.415	2.430	2.497	2.464	2.462	2.434
	2.381	2.414	2.469	2.447	2.440	2.420
$I_2P^+(PI_2)_2$	2.379	2.373	2.454	2.422	2.417	2.388
<b><math>P_2I_5^+</math></b>						
P–P	2.218	2.253	2.390	2.344	—	—
$I_3P^+-PI_2$	2.420	2.413	2.464	2.442	—	—
$I_3P^+-PI_2$	2.402	2.376	2.458	2.422	—	—

<sup>a</sup> Experimental data stem from the cations in **2** and in  $P_2I_5AlI_4$ . <sup>b</sup> TZVPP basis set. <sup>c</sup> SVP basis set. <sup>d</sup> 6-311G(2df) for P and SDD(spdf) for I.

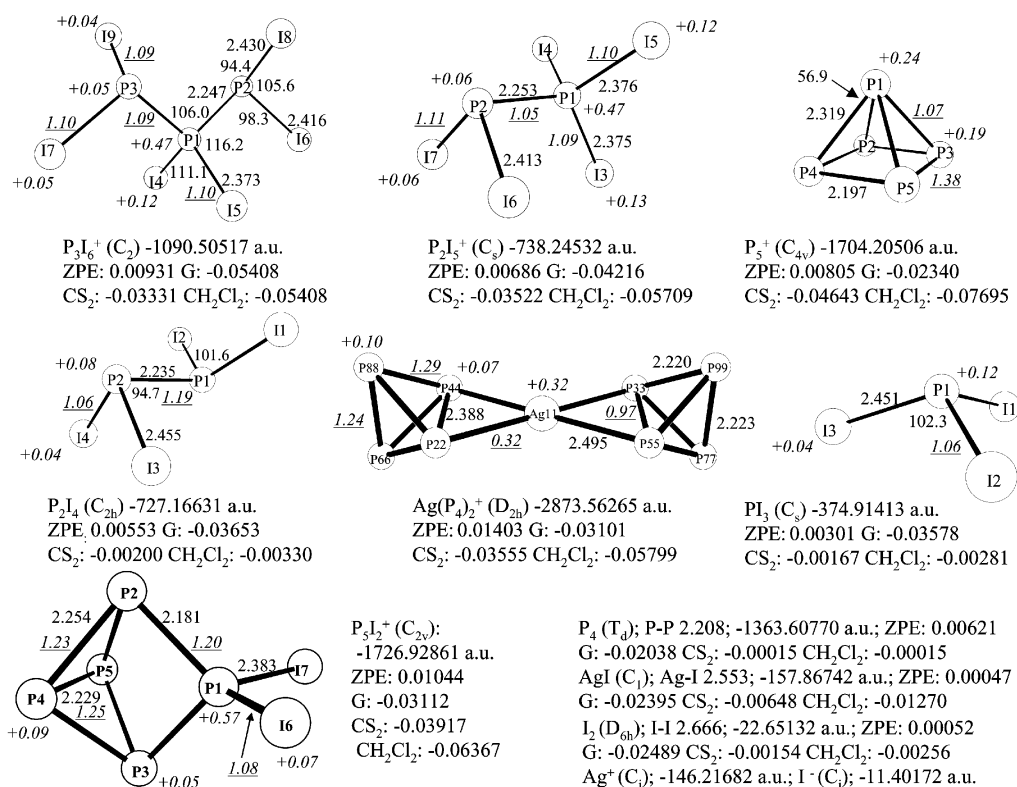


**Fig. 11** Fully optimised geometries, atomic energies and zero point energies (= ZPE), thermal corrections<sup>40</sup> to the free enthalpy at 298 K (= G), solvation energies<sup>39</sup> in CS<sub>2</sub> (= CS<sub>2</sub>) or CH<sub>2</sub>Cl<sub>2</sub> (= CH<sub>2</sub>Cl<sub>2</sub>) of several binary P–I species,  $Ag(P_4)_2^+$ ,  $P_5^+$ ,  $P_4$ ,  $I_2$  and AgI at the (RI-)MP2/TZVPP level. Computed partial charges are given in italics, shared electron numbers are shown in italics and underlined. All species included are true minima with no imaginary frequencies.

The quality of the data collected in Fig. 11 is further established by comparison to the experimental geometries of  $P_4$ ,  $P_2I_4$ ,  $PI_3$ ,  $I_2$  and AgI: observed and calculated parameters differ by a maximum of  $-0.020$  Å and  $+1.1^\circ$ . The geometries of  $Cl_2P(CHCl_2)_2^+$  and  $CHCl_3$  were also optimised at the MP2/TZVPP level.<sup>25,26</sup>

**Computationally assessed thermochemical properties.** For the estimation of thermochemical properties of reactions of the presented species and as an input for Born–Fajans–Haber cycle calculations we derived the enthalpies of formation of several species based on the accurate MP2/TZVPP calculations. For applications see ref. 27. ZPE energies were included in all cases. Known enthalpies of formation were taken from the literature.<sup>5,11</sup> [(g) = gaseous]

$\Delta_f H(P_5^+ (g))$  followed from the reaction enthalpy of  $P_3^+$  with  $0.5 P_4$  ( $\Delta_r H = -120$  kJ mol<sup>-1</sup>) as:

$$\begin{aligned} \Delta_f H(P_5^+ (g)) &= \Delta_f H(P_3^+ (g)) + [0.5 \times \Delta_f H(P_4 (g))] \\ &= 1006 + (0.5 \times 54) - 120 = \mathbf{913 \text{ kJ mol}^{-1}} \end{aligned}$$

This may be compared to the experimental  $\Delta_f H(P_4^+ (g))$  of 942 kJ mol<sup>-1</sup>.<sup>28</sup>  $\Delta_f H(Ag(P_4)_2^+ (g))$  followed from the enthalpy of reaction of  $Ag(P_4)_2^+ (g)$  giving  $Ag^+ (g)$  and  $2 P_4 (g)$  ( $\Delta_r H = -341$  kJ mol<sup>-1</sup>) as:

$$\begin{aligned} p\Delta_f H(Ag(P_4)_2^+ (g)) &= \Delta_f H(Ag^+ (g)) + [2 \times \Delta_f H(P_4 (g))] \\ &= 1017 + (2 \times 54) - 341 = \mathbf{784 \text{ kJ mol}^{-1}} \end{aligned}$$

$\Delta_f H(P_3I_6^+ (g))$  followed from the enthalpy of reaction of  $Ag^+ (g) + 1.5 P_2I_4 (g) + 0.5 I_2 (g) \rightarrow P_3I_6^+ (g) + AgI (g)$  ( $\Delta_r H = -212$  kJ mol<sup>-1</sup>) as:

$$\begin{aligned} \Delta_f H(P_3I_6^+ (g)) &= [1.5 \times \Delta_f H(P_2I_4(g))] + \Delta_f H(Ag^+(g)) + \\ &= [1.5 \times -4.7] + 1017 + [0.5 \times 62.4] - 135 - 212 \\ &= \mathbf{694 \text{ kJ mol}^{-1}} \end{aligned}$$

$\Delta_f H(P_2I_5^+ (g))$  followed from the enthalpy of reaction of eqn. (g) in Table 5 ( $\Delta_r H = +45$  kJ mol<sup>-1</sup>) as:

$$\Delta_f H(\text{P}_5\text{I}_5^+) (\text{g}) = \Delta_f H(\text{P}_3\text{I}_6^+) (\text{g}) - [0.25 \times \Delta_f H(\text{P}_2\text{I}_4 (\text{g}))] - [0.125 \times \Delta_f H(\text{P}_4 (\text{g}))] + 45 \text{ kJ mol}^{-1} = 694 - [0.25 \times -4.7] - [0.125 \times 54] + 45 = 733 \text{ kJ mol}^{-1}$$

$\Delta_f H(\text{P}_5\text{I}_2^+) (\text{g})$  followed from the enthalpy of reaction of eqn. (f) in Table 5 ( $\Delta_r H = -49 \text{ kJ mol}^{-1}$ ) as:

$$p\Delta_f H(\text{P}_5\text{I}_2^+) (\text{g}) = \Delta_f H(\text{P}_3\text{I}_6^+) (\text{g}) + \Delta_f H(\text{P}_4 (\text{g})) - \Delta_f H(\text{P}_2\text{I}_4 (\text{g})) + 49 \text{ kJ mol}^{-1} = 694 + 54 - (-4.7) + 49 = 792 \text{ kJ mol}^{-1}$$

## Discussion

### Establishing the nature of $\text{P}_5\text{I}_2^+$ : $^{31}\text{P}$ -NMR and Raman spectra

One comment prior to discussion: It is not adequate to calculate the  $^{31}\text{P}$ -NMR chemical shifts of the P–I cations by the standard procedures built in many quantum chemical program codes due to relativistic effects.<sup>29,30</sup> Iodine substituents at tetra-coordinate phosphorus atoms lead to a very pronounced relativistic upfield shift that may reach several hundred ppm.<sup>29,30</sup>

The connectivity of the novel  $\text{P}_5$  cage within  $\text{P}_5\text{I}_2^+$  followed unequivocally from the coupling pattern and integration of the first order  $^{31}\text{P}$ -NMR spectrum (Fig. 1). The  $C_{2v}$  symmetric  $\text{P}_5$  cage of the cation is without precedence and was not found as part of the many polyphosphides or organopolyphosphanes known to date.<sup>31</sup> However, it still remained to be established that the single phosphorus atom  $\text{P}_A$  bears two iodine atoms. A  $\text{P}_5^+$  cation with the same  $C_{2v}$  cage structure could be ruled out based on the calculated high MP2/TZVPP relative energies (including solvation energies) and the calculated  $^{31}\text{P}$ -NMR shifts for these species, even when the coordination of one or two molecules of  $\text{CH}_2\text{Cl}_2$  in several possible geometries was assumed.<sup>32</sup> Moreover  $C_{2v}$ - $\text{P}_5^+$  and its  $\text{CH}_2\text{Cl}_2$  solvates are not true minima but transition states or saddle points with imaginary frequencies (see Fig. 12).<sup>33</sup>

The dicoordinate formally positively charged single  $\text{P}_A$  atom in  $C_{2v}$ - $\text{P}_5^+$  would be expected to resonate somewhere between +1000 and +300 ppm,<sup>32</sup> depending on the number,  $n$ , of  $\text{CH}_2\text{Cl}_2$  molecules in  $\text{P}_5^+(\text{CH}_2\text{Cl}_2)_n$  ( $n = 0, 1, 2$ , several isomers). However, Table 3 shows that  $\delta^{31}\text{P}(\text{P}_A$  in **3**) is at considerably higher field at  $-89.0$  ppm. This is in the middle of the values observed in  $\text{P}_3\text{I}_6^+$  ( $-4.6$  ppm) with two electron-withdrawing  $\text{PI}_2$  units attached to  $\text{P}_A$  and that of  $\text{P}_A$  in  $\text{P}_2\text{I}_5^+$  which bears a third iodine atom which further shifts<sup>29</sup> the signal to higher field (to  $-142$  or  $-156.2$  ppm, see Table 3). Therefore the position of the electron-rich substituted  $\text{PI}_2^+$  unit in  $\text{P}_5\text{I}_2^+$  at  $\delta^{31}\text{P} = -89.0$  is very reasonable (electron donating bicyclobutane- $\text{P}_4$  moiety). Moreover the rather large  $^1J_{\text{PP}}$  couplings of the three  $\text{P}_A$  atoms in the P–I cations are in the same range, cf. 278.5 Hz in  $\text{P}_5\text{I}_2^+$ , 320.2 Hz in  $\text{P}_2\text{I}_5^+$  and 385.5 Hz in  $\text{P}_3\text{I}_6^+$  (Table 3). The chemical shifts of the atoms of the naked  $\text{P}_4$  unit in **3** can only be compared to metal–tetraphosphabicyclobutane

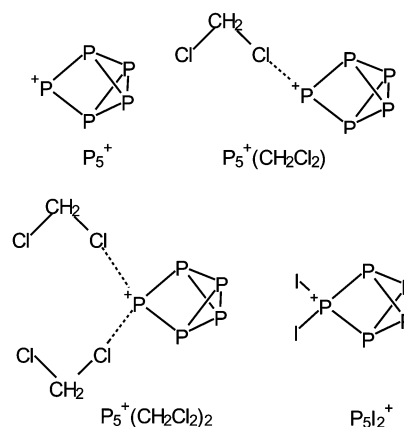


**Fig. 12** Computationally assessed possible unsolvated and solvated  $C_{2v}$ - $\text{P}_5^+$  structures. Only one of several examined  $\text{P}_5^+(\text{CH}_2\text{Cl}_2)_n$  isomers is schematically shown ( $n = 0, 1, 2$ ).

units since a similar  $\text{P}_5$  cage is unknown. However, the electro-positive  $\text{Cp}_2\text{M}$  ( $\text{M} = \text{Zr}, \text{Hf}$ ) groups  $\text{Z}^{34}$  in Table 3 are good substitutes for the  $\text{PI}_2^+$  unit in  $\text{P}_5\text{I}_2^+$  and chemical shifts of  $\text{P}_B$  and  $\text{P}_C$  as well as the smaller  $^1J_{\text{PBC}}$  coupling constants in  $\text{Cp}^*_2\text{HfP}_4$ ,<sup>34</sup>  $\text{Cp}^*_2\text{ZrP}_4$ <sup>34</sup> and  $\text{P}_5\text{I}_2^+$  match very well (Table 3).

Raman spectroscopy is also in agreement with the assignment of **3** as  $\text{P}_5\text{I}_2[\text{Al}(\text{OR})_4]$ . Observed and calculated vibrational frequencies are in very good agreement and are assigned in Table 4.

The presence of the intact  $\text{Al}(\text{OR})_4^-$  anion followed from the characteristic bands at 796, 745, 318 and 234  $\text{cm}^{-1}$  which are very similar to those observed in  $\text{Ag}(\text{P}_4)_2[\text{Al}(\text{OR})_4]^-$  (Table 4). Anion decomposition and  $(\text{RO})_3\text{Al}-\text{F}-\text{Al}(\text{OR})_3^-$  formation leads to new signals and a different pattern of the bands around 800  $\text{cm}^{-1}$ .<sup>35</sup> The presence of a  $\text{PI}_2$  moiety in **3** is evident from the very intense 100% band at 168  $\text{cm}^{-1}$  which is assigned to a  $\text{PI}_2$  stretching mode (cf.  $\text{PI}_4\text{AlCl}_4$ : 169  $\text{cm}^{-1}$ ,  $\text{A}_1$  mode of  $\text{PI}_4^+$ , 100% relative intensity<sup>36</sup>). According to the MP2 calculation, the position of the symmetric and antisymmetric  $\text{PI}_2$  stretches at 169 and 170  $\text{cm}^{-1}$  are indistinguishable with the 4  $\text{cm}^{-1}$  resolution of the spectrum and, therefore, occur at the same position which also may account for the high intensity of this band. 10 of the 15 expected vibrational bands of the cation were observed and all bands of the  $\text{P}_5$  cage are strongly mixed. The symmetric breathing mode of the  $\text{P}_5$  cage ( $\text{A}_1$ , 541  $\text{cm}^{-1}$ ) is slightly weakened if compared to the  $\text{A}_1$  mode of  $\text{P}_4$  (600  $\text{cm}^{-1}$ ) but higher in energy than the P–P vibrations of red phosphorus (highest energy band at 461  $\text{cm}^{-1}$ ).

### Stability and decomposition of the $\text{Al}(\text{OR})_4^-$ anion. Formation of **1** and **2**

Previous attempts to prepare  $\text{P}_2\text{I}_5^+$  salts by reaction of  $\text{I}_3^+\text{MF}_6^-$  ( $\text{M} = \text{As}, \text{Sb}$ ) with  $\text{P}_2\text{I}_4$  in various solvents failed and led to

**Table 3** Comparison of the  $^{31}\text{P}$ -NMR shifts of  $\text{P}_5\text{I}_2^+$  and  $\text{P}_3\text{I}_6^+$  with other relevant species

Z/Cation	$\delta\text{P}_A$	$\delta\text{P}_B$	$\delta\text{P}_C$	$\delta\text{P}_D$	$^1J_{\text{PAB}}$	$^1J_{\text{PBC}}$	$^1J_{\text{PAD}}$
$\text{Cp}^*_2\text{Hf}^{34}$	—	117.5	-219.3	—	—	193.9	—
$\text{Cp}^*_2\text{Zr}^{34}$	—	93.3	-214.0	—	—	201.1	—
$\text{I}_2\text{P}^+$ <b>3</b>	-89.0	168.2	-193.9	—	278.5	152.6	—
$\text{P}_3\text{I}_6^+$ <b>4</b>	-4.6	—	—	89.2	—	—	385.5
$\text{P}_2\text{I}_5\text{Al}_4$ (MAS) <sup>22</sup>	-142	—	—	114	—	—	—
$\text{P}_2\text{I}_5[\text{Al}(\text{OR})_4]^\text{a}$	-156.2	—	—	125.5	—	—	320.2

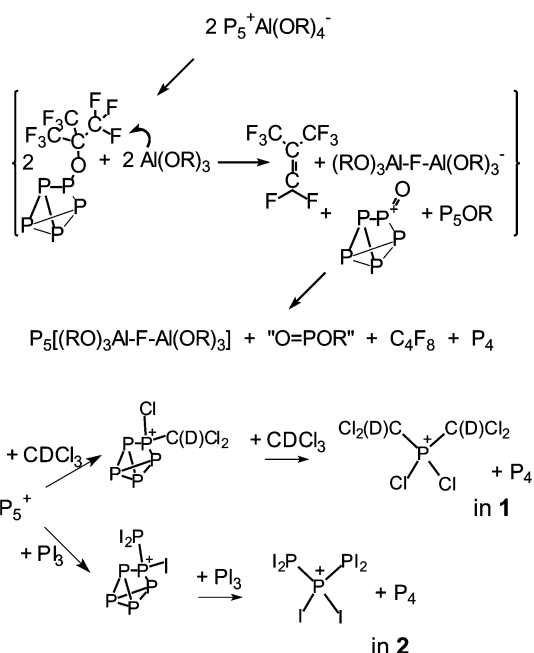
<sup>a</sup> From Fig. 2.

**Table 4** Experimental and non-scaled calculated vibrational frequencies of **3**

$\nu_{\text{exp.}}^a$ (% intensity)	$\nu_{\text{calc.}}^b$	Symmetry	Assignment
796 (21)			Al–O {cf. 798 in $\text{Ag}(\text{P}_4)_2[\text{Al}(\text{OR})_4]$ }
745 (20)			Al–O {cf. 746 in $\text{Ag}(\text{P}_4)_2[\text{Al}(\text{OR})_4]$ }
541 (32)	544	$A_1$	$\nu_s$ “breathing mode” of the $\text{P}_5$ cage
Within $A_1$ at 541?	537	$B_1$	$\nu_{\text{as}}$ P2–P1–P3
502 (20)	505	$A_1$	$\nu_s$ $\text{P}_5$ cage
Within $B_1$ at 448?	450	$B_2$	$\nu_{\text{as}}$ P2,3,1 and I1,2
448 (10)	444	$B_1$	$\nu_{\text{as}}$ P2,3,4,5
385 (30)	390	$B_1$	$\nu_{\text{as}}$ $\text{P}_5$ cage
359 (sh)	357	$A_2$	$\nu_{\text{as}}$ P2,3,4,5
354 (80)	350	$A_1$	$\nu_s$ P2,3,4,5
329 (70)	314	$A_1$	$\nu_{\text{as}}$ $\text{P}_5$ cage
318 (sh)			Anion {cf. 322 in $\text{Ag}(\text{P}_4)_2[\text{Al}(\text{OR})_4]$ }
234 (4)			Anion {cf. 234 in $\text{Ag}(\text{P}_4)_2[\text{Al}(\text{OR})_4]$ }
Within $A_1$ at 168?	170	$B_1$	$\nu_{\text{as}}$ $\text{PI}_2$ unit
168 (100)	169	$A_1$	$\nu_s$ $\text{PI}_2$ unit
126 (4)	132	$B_2$	P2–P1–P3 bend
87 (4)	86	$A_1$	$\text{PI}_2$ bend
n.o.	79	$A_2$	Cage deformation
n.o.	56	$B_1$	Cage deformation

<sup>a</sup> n.o. = not observed. <sup>b</sup> MP2/TZVPP frequencies.

decomposition and formation of  $\text{PF}_3$ ,  $\text{I}_2$  and  $\text{MI}_3$ .<sup>22</sup> The characterisation of **3** and **4** is therefore remarkable and demonstrated the stability of the  $\text{Al}(\text{OR})_4^-$  anion in comparison to the classical  $\text{MF}_6^-$  class of ions. Moreover,  $\text{Al}(\text{OR})_4^-$  salts are soluble in  $\text{CH}_2\text{Cl}_2$  even at very low temperatures ( $-90^\circ\text{C}$ ) which allowed the variable temperature NMR studies to be undertaken. However, at temperatures above  $-30^\circ\text{C}$  to rt following decomposition reactions of the  $\text{Al}(\text{OR})_4^-$  anion which led to the formation of the fluoride bridged  $(\text{RO})_3\text{Al}-\text{F}-\text{Al}(\text{OR})_3^-$  species indicated that cations such as  $\text{P}_5^+$  or  $\text{P}_5\text{I}_2^+$  and  $\text{P}_3\text{I}_6^+$  are very strong electrophiles. A possible hypothetical but balanced mechanism for the formation of the fluoride bridged anion in **1** and **2** and the subsequent insertion reactions starting from  $\text{P}_5^+$  is outlined in Scheme 1.



**Scheme 1** Hypothetical decomposition pathway leading to **1** and **2** [R = C(CF<sub>3</sub>)<sub>3</sub>].

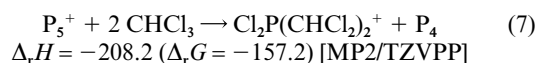
The first step of this decomposition reaction is possibly the abstraction of one OR ligand from  $\text{Al}(\text{OR})_4^-$ . Since  $\text{Al}(\text{OR})_3$  was shown to be a very strong Lewis acid<sup>8</sup> and the Al–F bond is the second strongest single bond in the Periodic table [BE =

$583 \pm 31 \text{ kJ mol}^{-1}$ ]<sup>37</sup> the subsequent fluoride ion abstraction from the generated  $\text{P}_5\text{OR}$  molecule close by appears likely. The fluoride ion abstraction is additionally aided by C=C (in  $\text{C}_4\text{F}_8$ ) and P=O (in  $\text{P}_5\text{O}^+$ ) double bond formation. In this step the fluoride bridged anion was formed. Subsequently the  $\text{P}_5\text{O}^+$  cation reacted with additional  $\text{P}_5\text{OR}$  present giving the  $\text{P}_5^+$  cation and other likely stable phosphorus containing species [“O=POR”, cf. O=POH;<sup>38</sup> that presumably dismutates to  $\text{P}_2\text{O}_3$  or  $\text{P}_2\text{O}_5$ ,  $\text{P}(\text{OR})_3$  and  $\text{P}_4$  (or  $\text{P}_{\text{red}}$ )]. The  $\text{P}_5^+$  cation then inserted into the C–Cl bond of  $\text{CDCl}_3$  (to give **1**) or  $\text{PI}_3$  (to give **2**).

The  $(\text{RO})_3\text{Al}-\text{F}-\text{Al}(\text{OR})_3^-$  anion has some similarity to the  $\text{Sb}_2\text{F}_{11}^-$  anion. For the latter species it was shown<sup>27</sup> that the fluoride ion affinity (= FIA) of 2  $\text{SbF}_5$  (l) (giving  $\text{Sb}_2\text{F}_{11}^-$ ) is greater than that of 1  $\text{SbF}_5$  (l) (giving  $\text{SbF}_6^-$ ) by  $70 \text{ kJ mol}^{-1}$ . Similarly it is clear that the FIA of 2  $\text{Al}(\text{OR})_3$  is greater than that of  $\text{Al}(\text{OR})_3$ . Therefore it is likely that only the combined power of 2  $\text{Al}(\text{OR})_3$  molecules is sufficient to abstract a fluoride ion [to form  $(\text{RO})_3\text{Al}-\text{F}-\text{Al}(\text{OR})_3^-$  and not two  $\text{F}-\text{Al}(\text{OR})_3^-$  anions]. The structural parameters of the  $(\text{RO})_3\text{Al}-\text{F}-\text{Al}(\text{OR})_3^-$  anion suggested that the fluoride bridged species is more stable (towards electrophilic attack) than the parent  $\text{Al}(\text{OR})_4^-$  ion, just as  $\text{Sb}_2\text{F}_{11}^-$  is more stable than  $\text{SbF}_6^-$ .<sup>27</sup>

#### Thermodynamics of the reaction of iodine with $\text{Ag}(\text{P}_4)_2^+$ , stability and formation of $\text{Cl}_2\text{P}(\text{CHCl}_2)_2^+$ , $\text{P}_5\text{I}_2^+$ and $\text{P}_3\text{I}_6^+$

In Scheme 1 we proposed that the  $\text{Cl}_2\text{P}(\text{CHCl}_2)_2^+$  cation was formed by the double insertion of the  $\text{P}^+$  unit of  $\text{P}_5^+$  into the C–Cl bond of chloroform, *i.e.*



A reaction according to eqn. (7) is both exothermic and exergonic and therefore likely to be the reason for the formation of the  $\text{Cl}_2\text{P}(\text{CHCl}_2)_2^+$  cation and also in agreement with the <sup>31</sup>P-NMR spectroscopic observation of excess  $\text{P}_4$ .

To understand the formation of  $\text{P}_5\text{I}_2^+$  and  $\text{P}_3\text{I}_6^+$  as opposed to that of  $\text{P}_5^+$  we assessed the underlying thermochemistry in the gas phase and in solution ( $\text{CS}_2$  and  $\text{CH}_2\text{Cl}_2$ ) by including approximate free solvation energies with the COSMO model.<sup>39</sup> All values given include the ZPE and thermal corrections to the enthalpy ( $H$ ) or the free energy ( $G$ )<sup>40</sup> at a temperature of 298 K [eqns. (a)–(j) in Table 5].

In the gas phase the enthalpy for the formation of  $\text{P}_5^+$  [eqn. (a)] is unfavourable by  $104.5 \text{ kJ mol}^{-1}$ . However, including entropy, solvation energies and considering the (expected)

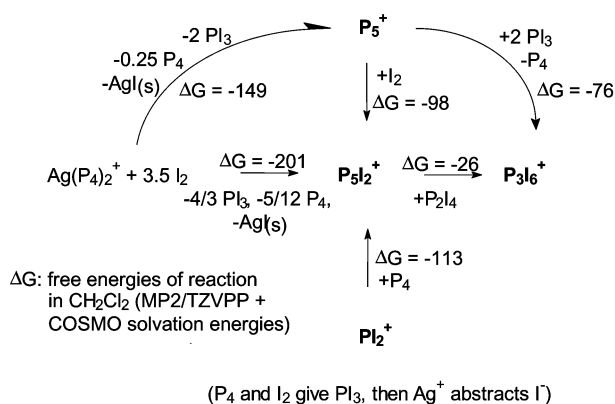


**Table 5** MP2/TZVPP enthalpies and free energies<sup>40</sup> of reaction (kJ mol<sup>-1</sup>) in the gas phase as well as CS<sub>2</sub> and CH<sub>2</sub>Cl<sub>2</sub> solution (COSMO model).<sup>39</sup> The values in parentheses include the formation of solid AgI

Reaction	$\Delta_r H(\text{gas})$	$\Delta_r G(\text{CS}_2)$	$\Delta_r G(\text{CH}_2\text{Cl}_2)$
(a) $\text{Ag}(\text{P}_4)_2^+ + 3.5 \text{I}_2 \rightarrow \text{P}_5^+ + 2 \text{PI}_3 + 0.25 \text{P}_4 + \text{AgI}$	+104.5 (-92.4) <sup>a</sup>	+48.7 (-131.2) <sup>b</sup>	+14.5 (-149.4) <sup>c</sup>
(b) $\text{Ag}(\text{P}_4)_2^+ + 3.5 \text{I}_2 \rightarrow \text{P}_5\text{I}_2^+ + 4/3 \text{PI}_3 + 5/12 \text{P}_4 + \text{AgI}$	-19.9 (-216.9) <sup>a</sup>	-20.3 (-200.2) <sup>b</sup>	-36.8 (-200.7) <sup>c</sup>
(c) $\text{P}_5^+ + 2 \text{PI}_3 \rightarrow \text{P}_3\text{I}_6^+ + \text{P}_4$	-205.8	-101.2	-75.8
(d) $\text{P}_5^+ + \text{I}_2 \rightarrow \text{P}_5\text{I}_2^+$	-184.8	-116.6	-98.1
(e) $\text{P}_4 + \text{PI}_2^+ \rightarrow \text{P}_5\text{I}_2^+$	-188.6	-123.6	-113.2
(f) $\text{P}_5\text{I}_2^+ + \text{P}_2\text{I}_4 \rightarrow \text{P}_3\text{I}_6^+ + \text{P}_4$	-49.0	-38.7	-25.7
(g) $\text{P}_2\text{I}_4 + \text{PI}_3 + \text{Ag}^+ \rightarrow \text{P}_3\text{I}_6^+ + \text{AgI}$	-197.8 (-394.7) <sup>a</sup>	-140.9 (-320.8) <sup>b</sup>	-115.2 (-278.8) <sup>c</sup>
(h) $\text{P}_2\text{I}_5^+ + \text{P}_2\text{I}_4 \rightarrow \text{P}_3\text{I}_6^+ + \text{PI}_3$	-20.3	-35.8	-32.5
(i) $\text{P}_3\text{I}_6^+ \rightarrow \text{P}_2\text{I}_5^+ + 0.25 \text{P}_2\text{I}_4 + 0.125 \text{P}_4$	45.4	30.9	27.1
(j) $\text{P}_3\text{I}_6^+ \rightarrow \text{P}_2\text{I}_5^+ + 1/3 \text{PI}_3 + 1/6 \text{P}_4$	53.8	29.2	25.3

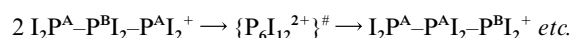
<sup>a</sup> The enthalpy for the process  $\text{AgI}(\text{g}) \rightarrow \text{AgI}(\text{s})$  is 196.9 kJ mol<sup>-1</sup>. <sup>b</sup> The enthalpy for the process  $\text{AgI}(\text{solv}) \rightarrow \text{AgI}(\text{s})$  in CS<sub>2</sub> is -179.9 kJ mol<sup>-1</sup>. <sup>c</sup> The enthalpy for the process  $\text{AgI}(\text{solv}) \rightarrow \text{AgI}(\text{s})$  in CH<sub>2</sub>Cl<sub>2</sub> is -163.6 kJ mol<sup>-1</sup>.

precipitation of solid AgI (s) favours the P<sub>5</sub><sup>+</sup> side and eqn. (a) is now exergonic by -131.2 to -149.4 kJ mol<sup>-1</sup>. P<sub>5</sub><sup>+</sup> formation is aided by solvation effects and more favourable in polar solvents such as CH<sub>2</sub>Cl<sub>2</sub>. In Scheme 1 we proposed that P<sub>3</sub>I<sub>6</sub><sup>+</sup> was formed by the double insertion of the P<sup>+</sup> unit of P<sub>5</sub><sup>+</sup> into the P-I bond of PI<sub>3</sub>. Eqn. (c) shows that this reaction is exergonic and therefore may be the reason for the formation of **2**. According to eqn. (b), starting with the same stoichiometry as eqn. (a), the direct formation of P<sub>5</sub>I<sub>2</sub><sup>+</sup> is exergonic. P<sub>5</sub>I<sub>2</sub><sup>+</sup> formation may proceed through the P<sub>5</sub><sup>+</sup> stage by reaction with excess I<sub>2</sub> [eqn. (d)] or alternatively through a PI<sub>2</sub><sup>+</sup> stage by insertion of the latter into the P-P bond of P<sub>4</sub> [eqn. (e)]. The PI<sub>2</sub><sup>+</sup> cation may have formed from Ag<sup>+</sup> and PI<sub>3</sub> which in turn originated from P<sub>4</sub> [from Ag(P<sub>4</sub>)<sub>2</sub><sup>+</sup>] and I<sub>2</sub>. In agreement with this proposal it was shown that P<sub>4</sub> and I<sub>2</sub> initially form PI<sub>3</sub> and only then P<sub>2</sub>I<sub>4</sub> (with excess P<sub>4</sub>)<sup>17</sup> and we observed PI<sub>3</sub> formation in eqn. (5) above. However, solely based on thermodynamics it can not be decided whether eqn. (d), eqn. (e) or yet another pathway is actually occurring. It may be noted though that in the case of formation of the Cl<sub>2</sub>P(CDCl<sub>2</sub>)<sub>2</sub><sup>+</sup> cation in **1** a PX<sub>2</sub><sup>+</sup> insertion pathway [X = Br, I; cf. eqn. (e)] must be excluded since the resulting cation would have to incorporate a PBr<sub>2</sub><sup>+</sup> unit which clearly is not the case. Therefore only the intermediate participation of a phosphorus cation such as P<sub>5</sub><sup>+</sup> explains the formation of **1** [eqn. (7)] and so P<sub>5</sub>I<sub>2</sub><sup>+</sup> formation as shown in eqn. (d) appears more likely, although eqn. (e) may be an alternative approach to synthesise P<sub>5</sub>I<sub>2</sub><sup>+</sup>.<sup>10,41</sup> In the *in situ* NMR reaction we observed that P<sub>5</sub>I<sub>2</sub><sup>+</sup> had already decomposed at -40 °C with formation of P<sub>3</sub>I<sub>6</sub><sup>+</sup>. Eqn. (f) gives a reasonable explanation for this reaction: at this temperature P<sub>2</sub>I<sub>4</sub>, formed from PI<sub>3</sub> and P<sub>4</sub> in the precipitate, becomes slightly soluble in CH<sub>2</sub>Cl<sub>2</sub> and therefore is available for a reaction with P<sub>5</sub>I<sub>2</sub><sup>+</sup> giving P<sub>3</sub>I<sub>6</sub><sup>+</sup> and P<sub>4</sub> (or P<sub>red</sub> since P<sub>2</sub>I<sub>4</sub> catalyses this transformation<sup>42</sup>). Scheme 2 summarises these findings.



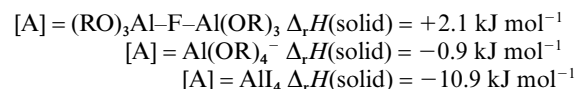
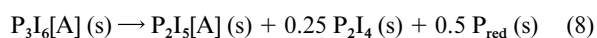
**Scheme 2** The reaction of Ag(P<sub>4</sub>)<sub>2</sub><sup>+</sup> with I<sub>2</sub> in CH<sub>2</sub>Cl<sub>2</sub> solution: Likely reaction pathways. All free energies are given in kJ mol<sup>-1</sup>. (s) = solid.

Eqn. (g) shows that the formation of P<sub>3</sub>I<sub>6</sub><sup>+</sup> starting from phosphorus iodides and Ag<sup>+</sup> is thermochemically possible. Fig. 2 suggested that P<sub>3</sub>I<sub>6</sub><sup>+</sup> in **4** was formed through P<sub>2</sub>I<sub>5</sub><sup>+</sup>, *i.e.* PI<sub>3</sub> reacted faster with Ag(CH<sub>2</sub>Cl<sub>2</sub>)[Al(OR)<sub>4</sub>] than P<sub>2</sub>I<sub>4</sub> and the P<sub>2</sub>I<sub>5</sub><sup>+</sup> formed reacted then with P<sub>2</sub>I<sub>4</sub> to give P<sub>3</sub>I<sub>6</sub><sup>+</sup> and PI<sub>3</sub>. Eqn. (h) is in agreement with this proposal and the small exergonic reaction energy of only -32.5 kJ mol<sup>-1</sup> (in CH<sub>2</sub>Cl<sub>2</sub>) and the low solubility of P<sub>2</sub>I<sub>4</sub> in cold CH<sub>2</sub>Cl<sub>2</sub> account for the slow P<sub>3</sub>I<sub>6</sub><sup>+</sup> formation [eqn. (6) above]. P<sub>3</sub>I<sub>6</sub><sup>+</sup> has a dynamic solution structure and coalesces at only 243 K ( $\Delta G^\ddagger = 38.8$  kJ mol<sup>-1</sup>). The transition state for the process that makes the two different P atoms in P<sub>3</sub>I<sub>6</sub><sup>+</sup> equivalent at rt is *not* the D<sub>3h</sub> symmetric three-membered ring *cyclo*-P<sub>3</sub>I<sub>6</sub><sup>+</sup> owing to the high relative energy of this species [ $E_{\text{rel}}(\text{cyclo-P}_3\text{I}_6^+) = +251$  kJ mol<sup>-1</sup> vs. C<sub>2</sub>-P<sub>3</sub>I<sub>6</sub><sup>+</sup> at the MP2/TZVPP level]. Less symmetric start geometries always led to the C<sub>2</sub> symmetric ground state and therefore it is most likely to assume a bimolecular exchange process for this reaction, *i.e.*:



However, different or additional exchange processes such as those outlined in eqns. (i) and (j) are also likely to be involved, especially since the experimental  $\Delta G^\ddagger$  and  $\Delta G(\text{CH}_2\text{Cl}_2)$  of eqns. (i) and (j) are on the same order of magnitude (38.8 vs. 25 to 27 kJ mol<sup>-1</sup>).

In contrast to P<sub>2</sub>I<sub>5</sub><sup>+</sup> (in P<sub>2</sub>I<sub>5</sub>AlI<sub>4</sub>) the P<sub>3</sub>I<sub>6</sub><sup>+</sup> cation was previously never observed with other anions such as AlI<sub>4</sub><sup>-</sup>. Therefore we investigated the stability of **2**, **4** and a hypothetical P<sub>3</sub>I<sub>6</sub>AlI<sub>4</sub>. Since gaseous disproportionation reactions according to eqns. (i) and (j) are still endothermic by 45 to 54 kJ mol<sup>-1</sup> this process has to be governed by lattice potential enthalpies. Therefore the solid state disproportionation [eqn. (8)] was assessed with three different anions, A, by a Born-Fajans-Haber calculation<sup>11</sup> which showed that P<sub>3</sub>I<sub>6</sub><sup>+</sup> is only stable with the large (RO)<sub>3</sub>-Al-F-Al(OR)<sub>3</sub><sup>-</sup> anion. With Al(OR)<sub>4</sub><sup>-</sup> its solid state stability is slightly unfavourable.



Since P<sub>4</sub> was never observed in solution a transformation of the P<sub>4</sub> molecule into red phosphorus (as catalysed by phosphorus iodides)<sup>42</sup> was assumed which additionally favoured the right hand side of eqn. (8) by 8.85 kJ mol<sup>-1</sup> (*i.e.*  $\Delta_r H$  for 1/4 P<sub>4</sub>(s) → P<sub>red</sub>(s) is 17.7 kJ mol<sup>-1</sup>).<sup>42</sup> Eqn. (8) provided evidence for our observation that the P<sub>3</sub>I<sub>6</sub><sup>+</sup> cation is only marginally stable and that—with many attempts—we were unable to obtain

single crystals of **4**. Rather **4** disproportionated giving  $\text{P}_2\text{I}_5[\text{Al}(\text{OR})_4]^{20}$  and  $\text{P}_2\text{I}_4$ . To obtain clean solid **4** one therefore has to quickly remove all volatiles of the diluted  $\text{CH}_2\text{Cl}_2$  solution and the thus obtained solid **4** appears to be metastable against a disproportionation as in eqn. (8).

## Conclusion

A series of reactions was performed that finally led to salts of the  $\text{P}_5\text{I}_2^+$  and  $\text{P}_3\text{I}_6^+$  cations. In some of the reactions the intermediate presence of naked polyphosphorus cations (e.g.  $\text{P}_5^+$ ) as concluded from the reaction products and *ab initio* calculations appeared likely. The phosphorus atoms in  $\text{P}_3\text{I}_6^+$  have an average oxidation state of 2.33 and this species is the first subvalent phosphorus P–X cation (X = H, F, Cl, Br, I) and a derivative of the as yet unknown subhalide  $\text{P}_3\text{I}_5$  (only  $\text{P}_3\text{F}_5$  was briefly characterised,<sup>43</sup> all other halides  $\text{P}_3\text{X}_5$  are unknown). This  $\text{P}_3\text{I}_6^+$  cation in **2** is only marginally stable in the solid state. The  $\text{P}_5\text{I}_2^+$  cation is the first example of a binary phosphorus rich P–X cation (X = halogen, H, organyl) and shows that this class of cations is accessible if provided with a suitable robust counterion such as  $\text{Al}(\text{OR})_4^-$ . Classical (oxidative) approaches to the  $\text{P}_n\text{I}_m^+$  ( $n \geq 2$ ) cations were earlier shown to be impossible since reactions always led to a complete fragmentation of the counterions  $\text{MF}_6^-$  (M = As, Sb). Moreover these classical routes only allow the isolation of oxidised but no subvalent species. This highlights the usefulness of the silver metathesis route employed here in combination with the new generation of spectator ions as exemplified by  $\text{Al}(\text{OR})_4^-$ . However, the decomposition of the latter anion in solution at temperatures above  $-30^\circ\text{C}$  to rt showed that even more stable counterions than  $\text{Al}(\text{OR})_4^-$  are needed. The fluoride bridged  $(\text{RO})_3\text{Al}-\text{F}-\text{Al}(\text{OR})_3^-$  anion appears to be a suitable candidate for this purpose. Currently we are investigating possible routes to the direct synthesis of silver salts of the latter anion.

## Experimental

All manipulations were performed using grease free Schlenk or dry box techniques and a dinitrogen or argon atmosphere. A drawing of the employed ‘‘Single Piece Apparatus’’ has been deposited as ESI. All apparatus were closed by J. Young valves and the solvents were rigorously dried over  $\text{P}_2\text{O}_5$  and degassed prior to use and stored under  $\text{N}_2$  on molecular sieves (4 Å). Yellow phosphorus was sublimed prior to use and dissolved in  $\text{CH}_2\text{Cl}_2$  or  $\text{CS}_2$  giving stock solutions which were manipulated by syringe techniques. The silver aluminate  $\text{Ag}(\text{CH}_2\text{Cl}_2)[\text{Al}(\text{OR})_4]$  and  $\text{Ag}(\text{P}_4)_2[\text{Al}(\text{OR})_4]$  were prepared according to the literature.<sup>8,9</sup> Raman spectra were recorded on a Bruker IFS 66v spectrometer equipped with the Raman model FRA106 and were obtained in the back scattering mode from solid samples sealed in a 5 mm NMR tube (1064 nm irradiation,  $4\text{ cm}^{-1}$  resolution). NMR spectra of sealed samples were run on a Bruker AC250 spectrometer and were referenced against the solvent ( $^1\text{H}$ ,  $^{13}\text{C}$ ) or external  $\text{H}_3\text{PO}_4$  ( $^{31}\text{P}$ ) and aqueous  $\text{AlCl}_3$  ( $^{27}\text{Al}$ ).

### Reaction leading to $\text{Cl}_2\text{P}(\text{CDCl}_2)_2^+[(\text{RO})_3\text{Al}-\text{F}-\text{Al}(\text{OR})_3]^-$ , **1**

$\text{Ag}(\text{CH}_2\text{Cl}_2)[\text{Al}(\text{OR})_4]$  (0.101 g, 0.087 mmol) was weighed into an NMR tube and  $\text{Br}_2$  (0.047 ml of a 0.942 M solution in  $\text{CS}_2$ , 0.0435 mmol) and  $\text{P}_4$  (0.41 ml of a 0.266 M solution in  $\text{CS}_2$ , 0.109 mmol) were added at rt with the exclusion of light. The brownish suspension was exposed to ultrasound for 5 minutes. All volatiles were removed in vacuum and the greyish–brown residue was dissolved in 0.5 ml of  $\text{CDCl}_3$  giving a brownish solution over little precipitate that appeared to be  $\text{AgBr}$ . The sample was sealed, NMR spectra were recorded and after two months a large amount of uniform colourless single crystals had formed. The unit cell of at least 10 crystals was determined and all of them were shown to be

$\text{Cl}_2\text{P}(\text{CDCl}_2)_2^+[(\text{RO})_3\text{Al}-\text{F}-\text{Al}(\text{OR})_3]^-$ , **1**, which therefore is seen as the major product of this reaction. NMR data of the solution:  $^{13}\text{C}$ -NMR (63 MHz,  $\text{CDCl}_3$ ,  $25^\circ\text{C}$ ):  $\delta = 120.8$  (q,  $\text{CF}_3$ ,  $J_{\text{CF}} = 291.2$  Hz);  $^{31}\text{P}$ -NMR (101 MHz,  $\text{CDCl}_3$ ,  $25^\circ\text{C}$ ):  $\delta = +144$  [s,  $\text{Cl}_2\text{P}(\text{CDCl}_2)_2^+$ , 10% of P content]  $-500$  (s,  $\text{P}_4$ , 90% of the P content).

### Reaction leading to $\text{P}_3\text{I}_6^+[(\text{RO})_3\text{Al}-\text{F}-\text{Al}(\text{OR})_3]^-$ , **2**

$\text{Ag}(\text{CH}_2\text{Cl}_2)[\text{Al}(\text{OR})_4]$  (0.624 g, 0.522 mmol) was weighed into a single piece apparatus<sup>44</sup> and  $\text{P}_4$  (1.72 ml of a 0.605 M solution in  $\text{CS}_2$ , 1.044 mmol) was added to the solid. All volatiles were removed in vacuum (slightly brownish residue). Solid  $\text{I}_2$  (0.465 g, 1.832 mmol) was weighed into the second bulb of the apparatus,  $\text{CH}_2\text{Cl}_2$  (10 ml) condensed onto the  $\text{P}_4/\text{Ag}(\text{CH}_2\text{Cl}_2)[\text{Al}(\text{OR})_4]$  mixture and subsequently all the iodine was sublimed onto the phosphorus containing side. The resulting orange solution over yellow precipitate was stirred overnight at  $-30^\circ\text{C}$ . All volatiles were removed in vacuum (theoretically expected weight of the residue: 1.174 g, found: 1.132 g) and the yellowish residue was extracted with 10 ml of  $\text{CS}_2$  at rt. From this yellow  $\text{CS}_2$  solution 0.501 g of a mixture of single crystals was obtained: orange needles of  $\text{P}_2\text{I}_4$  (unit cell determination) and yellow extremely sensitive plates of  $\text{P}_3\text{I}_6^+[(\text{RO})_3\text{Al}-\text{F}-\text{Al}(\text{OR})_3]^-$ , **2** (X-ray). A Raman spectrum of this mixture only showed the bands of  $\text{P}_2\text{I}_4$  (which in comparison to **2** is a very good Raman scatterer<sup>18</sup> and therefore prevents the observation of the weak  $\text{P}_3\text{I}_6^+$  bands). NMR data of the  $\text{CS}_2$  solution:  $^{13}\text{C}$ -NMR (63 MHz,  $\text{CS}_2$ – $\text{CD}_2\text{Cl}_2$ ,  $25^\circ\text{C}$ ):  $\delta = 122.2$  (q,  $\text{CF}_3$ ,  $J_{\text{CF}} = 290.6$  Hz);  $^{27}\text{Al}$ -NMR (78 MHz,  $\text{CS}_2$ – $\text{CD}_2\text{Cl}_2$ ,  $25^\circ\text{C}$ ):  $\delta = 34.0$  (s,  $\nu_{1/2} = 28$  Hz);  $^{31}\text{P}$ -NMR (101 MHz,  $\text{CS}_2$ – $\text{CD}_2\text{Cl}_2$ ,  $25^\circ\text{C}$ ):  $\delta = 176$  ( $\nu_{1/2} = 2100$  Hz), 105 ( $\nu_{1/2} = 1600$  Hz);  $^{31}\text{P}$ -NMR (101 MHz,  $\text{CS}_2$ – $\text{CD}_2\text{Cl}_2$ ,  $-30^\circ\text{C}$ ):  $\delta = 175.5$  ( $\nu_{1/2} = 5$  Hz), 104.5 ( $\nu_{1/2} = 5$  Hz);  $^{31}\text{P}$ -NMR (101 MHz,  $\text{CS}_2$ – $\text{CD}_2\text{Cl}_2$ ,  $-70^\circ\text{C}$ ):  $\delta = 175.7$  ( $\nu_{1/2} = 4$  Hz), 103.9 ( $\nu_{1/2} = 4$  Hz).

### NMR reaction leading to $\text{P}_5\text{I}_2^+[\text{Al}(\text{OR})_4]^-$ , **3**

$\text{Ag}(\text{P}_4)_2^+[\text{Al}(\text{OR})_4^-]$  (0.151 g, 0.114 mmol) was weighed into an NMR tube connected to a valve.  $\text{I}_2$  (0.101 g, 0.399 mmol) was sublimed onto the solid at 77 K after which 0.9 ml of  $\text{CD}_2\text{Cl}_2$  was condensed onto the mixture. The NMR tube was sealed and then placed in a dry ice–isopropanol bath and activated with ultrasound at  $-78^\circ\text{C}$  for about 10 minutes. The initial  $^{31}\text{P}$ -NMR spectra were run 30 minutes later and the  $^{13}\text{C}$ - and  $^{27}\text{Al}$ -NMR spectra after storage at  $-80^\circ\text{C}$  one week later (no decomposition visible in the  $^{31}\text{P}$ -NMR).  $^{13}\text{C}$ -NMR (63 MHz,  $\text{CD}_2\text{Cl}_2$ ,  $-90^\circ\text{C}$ ):  $\delta = 122.4$  (q,  $\text{CF}_3$ ,  $J_{\text{CF}} = 290.1$  Hz);  $^{27}\text{Al}$ -NMR (78 MHz,  $\text{CD}_2\text{Cl}_2$ ,  $-90^\circ\text{C}$ ):  $\delta = 39.5$  (s,  $\nu_{1/2} = 27$  Hz);  $^{31}\text{P}$ -NMR (101 MHz,  $\text{CD}_2\text{Cl}_2$ ,  $-90^\circ\text{C}$ ):  $\delta = 168.2$  (2P, dt,  $^1J_{\text{P}_2,3-\text{P}_1} = 278.5$  Hz,  $^1J_{\text{P}_2,3-\text{P}_4,5} = 152.6$  Hz),  $-89.0$  (1P, tt,  $^1J_{\text{P}_1-\text{P}_2,3} = 278.5$  Hz,  $^2J_{\text{P}_1-\text{P}_4,5} = 26.7$  Hz),  $-193.9$  (2P, td,  $^1J_{\text{P}_4,5-\text{P}_2,3} = 152.6$  Hz,  $^2J_{\text{P}_4,5-\text{P}_1} = 26.7$  Hz). Upon overnight warming to  $-40^\circ\text{C}$  the  $\text{P}_5\text{I}_2^+$  signals vanished and, apart from other unassigned signals of lower intensity, those of  $\text{P}_3\text{I}_6^+$  appeared as the major P-containing peaks [ $\delta^{31}\text{P}(-80^\circ\text{C}) = 89.2$  (2P, d,  $^1J_{\text{pp}} = 385.5$  Hz),  $-4.6$  (1P, t,  $^1J_{\text{pp}} = 385.5$  Hz)].

### Synthesis of $\text{P}_5\text{I}_2^+[\text{Al}(\text{OR})_4]^-$ , **3**

$\text{Ag}(\text{P}_4)_2^+[\text{Al}(\text{OR})_4^-]$  (1.020 g, 0.765 mmol) was weighed into a two bulbed vessel incorporating a sintered glass frit and stopped by J. Young valves.  $\text{I}_2$  (0.697 g, 2.746 mmol) was sublimed onto the solid at 77 K after which 5 ml of  $\text{CH}_2\text{Cl}_2$  were condensed onto the mixture. The apparatus was placed in a dry ice–isopropanol bath until the solvent had thawed and was then stored in a  $-80^\circ\text{C}$  freezer and every 30 minutes heavily shaken for about one minute (10 times). After four days at  $-80^\circ\text{C}$  the yellow solution over a yellow–orange precipitate was filtered at  $-80^\circ\text{C}$ . All volatiles were then quickly removed at about  $0^\circ\text{C}$  (expected weight of the material: 1.717 g, found: 1.737 g) and

the apparatus immediately transferred into a glove box. Soluble yellow  $\text{P}_5\text{I}_2^+[\text{Al}(\text{OR})_4^-]$ , **3** [0.963 g (0.700 mmol), expected: 1.052 g; yield: 92%] and 0.611 g insoluble material (expected: 0.665 g) were isolated while 0.140 g were not accessible within the flask (total: 0.963 g + 0.611 g + 0.140 g = 1.714 g; expected: 1.717 g). Raman spectra of **3** (see Table 4) and the insoluble material ( $\text{P}_4$ ,  $\text{PI}_3$  and traces of  $\text{P}_2\text{I}_4$ ) were recorded immediately after sample preparation. A  $^{31}\text{P}$ -NMR sample of yellow **3** in  $\text{CD}_2\text{Cl}_2$  gave the same spectrum as the one observed in the *in situ* reaction above. Elemental analysis for  $\text{P}_5\text{I}_2^+[\text{Al}(\text{OR})_4^-]$  ( $\text{C}_{16}\text{Al}_1\text{F}_{36}\text{I}_2\text{O}_4\text{P}_5$ ): found I 18.7, calc. I 18.5%.

#### NMR scale synthesis of $\text{P}_3\text{I}_6^+[\text{Al}(\text{OR})_4^-]$ , **4**

$\text{Ag}(\text{CH}_2\text{Cl}_2)[\text{Al}(\text{OR})_4]$  (0.110 g, 0.095 mmol),  $\text{PI}_3$  (0.040 g, 0.097 mmol) and  $\text{P}_2\text{I}_4$  (0.054 g, 0.095 mmol) were weighed into a NMR tube attached to a valve. 1.0 ml of  $\text{CD}_2\text{Cl}_2$  was condensed onto the mixture at 77 K and the tube was flame sealed *in vacuo*. Upon warming an orange solution and  $\text{AgI}$  precipitate formed at low temperatures. The mixture was heavily shaken for 15 minutes after which all visible phosphorus iodides were consumed. The tube was then stored at  $-78^\circ\text{C}$  until the NMR spectra were recorded 12 h later ( $\text{P}_2\text{I}_5^+$  and  $\text{P}_3\text{I}_6^+$  present). Another NMR run after 14 d storage at  $-30^\circ\text{C}$  showed that only  $\text{P}_3\text{I}_6^+$  was present (NMR data given in text).

#### Synthesis of $\text{P}_3\text{I}_6^+[\text{Al}(\text{OR})_4^-]$ , **4**

$\text{PI}_3$  (0.205 g, 0.498 mmol),  $\text{P}_2\text{I}_4$  (0.286 g, 0.502 mmol) and  $\text{CH}_2\text{Cl}_2$  (5 ml) were added into one bulb of a single piece apparatus.<sup>44</sup> This mixture was cooled to  $-78^\circ\text{C}$  when  $\text{Ag}(\text{CH}_2\text{Cl}_2)[\text{Al}(\text{OR})_4]$  (11.3 ml of a 0.0443 M solution in  $\text{CH}_2\text{Cl}_2$ , 0.500 mmol) were slowly added. An orange solution and  $\text{AgI}$  precipitate formed at low temperatures ( $-78^\circ\text{C}$ ). The stirred mixture was allowed to reach room temperature within 30 minutes and after an additional 30 minutes all visible phosphorus iodides were consumed. The apparatus was then stored for 4 days at  $-30^\circ\text{C}$  after which a  $^{31}\text{P}$ -NMR sample of the solution was prepared from a special outlet. This NMR spectrum showed  $\text{P}_3\text{I}_6^+$  to be the only P-containing species present and, therefore, the mixture was filtered. The insoluble precipitate ( $\text{AgI}$ , found: 0.120 g, calc.: 0.117 g) was washed several times (back condensing of  $\text{CH}_2\text{Cl}_2$ ) and then all volatiles of the filtrate were quickly removed *in vacuo* leaving a yellow powder of **4** (0.724 g, 79%). Raman samples prepared from this powder rapidly decomposed in the beam of the laser with all conditions checked. NMR data and analysis of yellow **4** in  $\text{CD}_2\text{Cl}_2$ :  $^{13}\text{C}$ -NMR (63 MHz,  $\text{CD}_2\text{Cl}_2$ ,  $25^\circ\text{C}$ ):  $\delta = 121.5$  (q,  $\text{CF}_3$ ,  $J_{\text{CF}} = 292.1$  Hz);  $^{27}\text{Al}$ -NMR (78 MHz,  $\text{CD}_2\text{Cl}_2$ ,  $25^\circ\text{C}$ ):  $\delta = 36.0$  (s,  $\nu_{1/2} = 22$  Hz);  $^{31}\text{P}$ -NMR (101 MHz,  $\text{CD}_2\text{Cl}_2$ ,  $25^\circ\text{C}$ ):  $\delta = 61$  ( $\nu_{1/2} = 1000$  Hz)  $^{31}\text{P}$ -NMR (101 MHz,  $\text{CD}_2\text{Cl}_2$ ,  $-90^\circ\text{C}$ ):  $\delta = 89.2$  (d,  $^1J_{\text{PP}} = 385.5$  Hz, 2 P),  $-4.6$  (t,  $^1J_{\text{PP}} = 385.5$  Hz, 1 P).  $\text{C}_{16}\text{Al}_1\text{F}_{36}\text{I}_6\text{O}_4\text{P}_3$ ; found I 41.4, calc. I 41.8%.

#### X-Ray crystal structure determinations

Data collections for X-ray structure determinations were performed on a STOE IPDS diffractometer using graphite-monochromated Mo-K $\alpha$  (0.71073 Å) radiation. Single crystals were mounted in perfluoroether oil on top of a glass fibre and then brought into the cold stream of a low temperature device so that the oil solidified. Crystals of **2** given to cooled ( $-20^\circ\text{C}$ ) dry perfluoroether or hydrocarbon oil decomposed very rapidly and from the fluorinated oil one had about 45 to 60 seconds to select a crystal, put it on top of the glass fibre and bring it onto the diffractometer. Of the approximately 15 crystals tested the one reported gave the best data set. All calculations were performed on PC's using the SHELX97 software package.<sup>50</sup> The structures were solved by direct methods and successive interpretation of the difference Fourier maps, followed by least-

**Table 6** Crystallographic data and refinement details

Compound	1	2
Crystal size/mm	0.3 × 0.4 × 0.5	0.05 × 0.3 × 0.3
Formula	$\text{C}_{26}\text{H}_2\text{Al}_2\text{Cl}_6\text{F}_{55}\text{O}_6\text{P}$	$\text{C}_{24}\text{Al}_2\text{F}_{55}\text{I}_6\text{O}_6\text{P}_3$
Formula weight	1752.91	2337.51
Crystal system	Triclinic	Triclinic
Space group	$P\bar{1}$	$P\bar{1}$
<i>a</i> /Å	12.781(3)	10.375(2)
<i>b</i> /Å	13.445(3)	10.757(2)
<i>c</i> /Å	16.561(3)	26.591(5)
<i>a</i> /°	88.45(3)	95.07(3)
<i>β</i> /°	69.56(3)	92.84(3)
<i>γ</i> /°	82.99(3)	98.48(3)
<i>V</i> /Å <sup>3</sup>	2646.3(9)	2917.6(10)
<i>Z</i>	2	2
$\rho$ (calc)/Mg m <sup>-3</sup>	2.200	2.661
$\mu$ /mm <sup>-1</sup>	0.625	3.521
Max./min. transmission	0.678/0.746	0.832/0.873
$2\theta$ /°	51.84	51.90
<i>T</i> /K	170	175
Reflections collected	20542	18169
Reflections unique	9396	10614
Reflections observed (4 $\sigma$ )	6929	2630
<i>R</i> (int)	0.0415	0.1850
GOOF	1.087	0.676
Final <i>R</i> (4 $\sigma$ )	0.1298	0.0744
Final <i>wR</i> 2	0.3729	0.1636
Largest residual peak/e Å <sup>-3</sup>	1.339	1.088

squares refinement. All atoms were refined anisotropically. The  $\text{P}_3\text{I}_6^+$  cation in **2** is disordered over two positions (0.865 to 0.135 occupancy) and only the major position is discussed in the text. The anions in **1–2** exhibit rotational disorder of the  $\text{CF}_3$  groups as well as the entire  $\text{C}(\text{CF}_3)_3$  groups. Therefore several fluorine and carbon atoms were split over two positions resulting in site occupation factors of 20–40%. Moreover a series of about 233 (**1**)/177 (**2**) SADI and FREE restraints had to be used in both structures to assign reasonable structural parameters to the  $\text{CF}_3$  groups. However, the cations in **1–2** were well behaved. The solid state packing of **2** was drawn with Diamond 2.1 (K. Brandenburg, Crystal Impact GbR, 1998). Relevant data concerning crystallography, data collection and refinement details are compiled in Table 6.

CCDC reference numbers 162636 and 162637.

See <http://www.rsc.org/suppdata/dt/b1/b103957c/> for crystallographic data in CIF or other electronic format.

#### Computational details

Initial calculations and the calculation of the thermal contributions to the enthalpy and free energy were performed with Gaussian98.<sup>45</sup> For P the 6-311G(2df) basis set was used and for I the SDD effective core potential augmented with one set of uncontracted s, p, d and f polarisation functions [= SDD-(spdf)]. Since it was realised that MP2 geometries were needed to give an accurate description of the species in question all further computations were done with the program TURBO-MOLE.<sup>46</sup> The geometries of all species were optimised at the (RI-)MP2 level<sup>47</sup> with the triple  $\zeta$  valence polarisation (one d and one f function) TZVPP basis set.<sup>48</sup> The 46 core electrons of I were replaced by a quasi-relativistic effective core potential. Approximate solvation energies ( $\text{CS}_2$  and  $\text{CH}_2\text{Cl}_2$  solution with  $\epsilon_r = 2.63$  and 8.92) were calculated with the COSMO model<sup>49</sup> at the BP86/SV(P) (DFT)-level using the MP2/TZVPP geometries. Frequency calculations were performed for all species and all structures represent true minima without imaginary frequencies on the respective hypersurface. For thermodynamic calculations the zero point energy and thermal contributions to the enthalpy or the free energy at 298 K have been included.<sup>40</sup> For selected species a modified Roby–Davidson population analysis has been performed using the MP2/TZVPP electron density.

## Acknowledgements

We thank Prof. H. Schnöckel and Prof. J. Passmore for valuable discussions and advice, Dipl. Chem. G. Stößer and Dipl. Chem. J. Bahlo for recording the Raman spectra and H. Berberich and Dr. E. Matern for recording the many low temperature NMR spectra. Financial support from the German science foundation DFG and the Fond der Chemischen Industrie are gratefully acknowledged.

## References and notes

- (a) T. P. Martin, *Z. Phys. D: At., Mol. Clusters*, 1986, **3**, 211; (b) R. Huang, H. Li, Z. Lin and S. Yang, *J. Phys. Chem.*, 1995, **99**, 1418; (c) R. B. Huang, Z. Y. Liu, P. Zhang, Y. B. Zhu, F. C. Lin, J. H. Zhao and L. S. Zheng, *Chin. J. Struct. Chem.*, 1993, **180**; (d) Z. Y. Liu, R. B. Huang and L. S. Zheng, *Z. Phys. D: At., Mol. Clusters*, 1996, **38**, 171.
- J. A. Zimmerman, S. B. H. Bach, C. H. Watson and J. R. Eyler, *J. Phys. Chem.*, 1990, **95**, 98.
- L.-S. Wang, B. Niu, Y. T. Lee and D. A. Shirley, *J. Chem. Phys.*, 1990, **93**, 6318.
- (a)  $P_n$  and  $P_n^+$ ,  $n = 1-8$ , R. O. Jones and D. Hohl, *J. Chem. Phys.*, 1990, **92**, 6710; (b)  $P_n$  and  $P_n^+$ ,  $n = 1-11$ , R. O. Jones and G. Seifert, *J. Chem. Phys.*, 1992, **96**, 7564; (c)  $E_n$  and  $E_n^+$ ,  $n = 1-11$ , E = P, As, R. O. Jones and P. Ballone, *J. Chem. Phys.*, 1994, **100**, 4941.
- See for example: (a) D. D. Wagman, W. H. Evans, V. B. Parker, R. H. Schumm, I. Halow, S. M. Bailey, K. L. Churney and R. L. Nuttall, *J. Phys. Chem. Ref. Data, Suppl.*, 1982, **11**, 2; (b) S. G. Lias, J. E. Bartmess, J. F. Liebman, J. L. Holmes, R. D. Levin and W. G. Mallard, *J. Phys. Chem. Ref. Data, Suppl.*, 1988, **17**, 1; (c) *CRC Handbook of Chemistry and Physics*, 76th edn., editor-in-chief D. R. Lide, CRC Press, Boca Raton, FL, 1986; (d) <http://www.nist.gov/chemistry>.
- J. D. Corbett, in *Progress in Inorganic Chemistry*, vol. 21, editor S. J. Lippard, John Wiley, New York, 1976, pp. 129–158.
- S. M. Ivanova, B. G. Nolan, Y. Kobayashi, S. M. Miller, O. P. Anderson and S. H. Strauss, *Chem. Eur. J.*, 2001, **7**, 503.
- I. Krossing, *Chem. Eur. J.*, 2001, **7**, 490.
- (a) I. Krossing, *J. Am. Chem. Soc.*, 2001, **123**, 4603; (b) I. Krossing and L. van Wüllen, *Chem. Eur. J.*, 2002, **8**, 700.
- I. Krossing and I. Raabe, *Angew. Chem.*, 2001, **113**, 4544.
- Data employed for the Born–Fajans–Haber cycle calculations (all enthalpies in  $\text{kJ mol}^{-1}$ ): (a) Lattice potential enthalpies were taken from the literature ( $\text{AgI}$ : 890.3)<sup>5c</sup> or estimated by Jenkins and Passmore's volume based modified Kapustinskii equation:<sup>12</sup>  $\text{Ag}[\text{Al}(\text{OR})_4] = 364$ ,  $\text{P}_2\text{I}_4[\text{Al}(\text{OR})_4] = 345$ ,  $\text{P}_3\text{I}_6[\text{Al}(\text{OR})_4] = 334$ ,  $\text{P}_2\text{I}_4[\text{Al}(\text{OR})_4] = 340$ ,  $\text{P}_3\text{I}_6[(\text{RO})_3\text{Al}-\text{F}-\text{Al}(\text{OR})_3] = 311$ ,  $\text{P}_2\text{I}_4[(\text{RO})_3\text{Al}-\text{F}-\text{Al}(\text{OR})_3] = 314$ ,  $\text{P}_2\text{I}_4[\text{AlI}_4] = 398$ ,  $\text{P}_3\text{I}_6[\text{AlI}_4] = 386$ . The thermochemical volume of  $\text{Al}(\text{OR})_4^-$  is  $725 \text{ \AA}^3$ ,  $\text{Ag}^+$  ( $4 \text{ \AA}^3$ ),  $\text{AlI}_4^-$  ( $244 \text{ \AA}^3$ ). The volumes of  $\text{P}_5^+$  [ $\approx 120 \text{ \AA}^3$ , with  $\text{S}_2\text{N}_2^+(97) < \text{P}_5^+ < \text{S}_2\text{Cl}_3^+(146)$ ],<sup>12</sup>  $\text{P}_2\text{I}_5^+$  [ $\approx 261 \text{ \AA}^3$ , from  $\text{V}(\text{P}_2\text{I}_5\text{AlI}_4) = 505^{21}$  and  $\text{V}(\text{AlI}_4^-)$  above],  $\text{P}_3\text{I}_6^+$  [ $\approx 330 \text{ \AA}^3$ , with  $\text{V}(\text{P}_3\text{I}_6^+) \approx 1.5 \cdot \text{V}(\text{P}_2\text{I}_4)$ ] and  $(\text{RO})_3\text{Al}-\text{F}-\text{Al}(\text{OR})_3^-$  [ $\approx 1129 \text{ \AA}^3$ , from  $\text{V}(\text{P}_3\text{I}_6[(\text{RO})_3\text{Al}-\text{F}-\text{Al}(\text{OR})_3]) = 1459$  and  $\text{V}(\text{P}_3\text{I}_6^+)$  above] were assessed/estimated; (b) Enthalpies of sublimation were taken from the literature ( $\text{P}_4$ : 54.4,  $\text{I}_2$ : 62.4) or were assessed [ $\text{P}_2\text{I}_4$ :  $\Delta H_{\text{sub}}(\text{P}_2\text{I}_4) = 83.0$ ; by computing the enthalpy of reaction for the process:  $0.5 \text{ P}_4 (\text{g}) + 2 \text{ I}_2 (\text{g}) \rightarrow \text{P}_2\text{I}_4 (\text{g})$ ;  $\Delta_r H = -156.7$  at the MP2/TZVPP level.  $\Delta_r H(\text{P}_4 (\text{g}))$ ,  $\Delta_r H(\text{I}_2 (\text{g}))$  (see below) and  $\Delta_r H(\text{P}_2\text{I}_4 (\text{s})) = -87.7$  are known]; (c) Enthalpies of formation were taken from the literature ( $\text{Ag}^+$ : 1017,  $\text{I}^-$  (g):  $-188.6$ ,  $\text{P}_4$  (g): 54.4,  $\text{I}_2$  (g): 62.4,  $\text{P}_3^+$  (g): 1006,  $\text{AgI}$  (g): 135) or assessed ( $\text{P}_2\text{I}_4$  (g):  $-4.7$ , MP2/TZVPP see above;  $\text{P}_5^+$  (g): 913; see text).
- H. K. Roobottom, H. D. B. Jenkins, J. Passmore and L. Glasser, *Inorg. Chem.*, 1999, **38**, 3609.
- We optimised the known<sup>4</sup> global minima of the  $\text{P}_n^+$  cations ( $n = 3, 5, 7$ ) at the BP86/SVP, B3LYP/TZVPP and MP2/TZVPP levels and also calculated the vibrational frequencies and Raman intensities (only BP86) of these species. The observed new P–P stretches ( $480$  to  $630 \text{ cm}^{-1}$ ) fell into a range calculated to be typical for these cations.
- Zdirad Zak and M. Cernik, *Acta Crystallogr., Sect. C*, 1996, **52**, 290.
- Similarly  $\text{CS}_2$  was used to remove excess  $\text{S}_8$  in highly electrophilic and oxidising sulfur cation or  $\text{S}_2\text{N}^+$  chemistry.
- We showed that solid  $\text{P}_4$  is also visible in a conventional solution NMR spectrometer due to the high local symmetry of the cubic solid  $\text{P}_4$  (see ref. 9b).
- B. W. Tattershall and N. L. Kendall, *Polyhedron*, 1994, **13**, 1517.
- As observed earlier, large counterions such as  $\text{Al}(\text{OR})_4^-$  lead to fluorescence and dilute the amount of Raman scatterer present (= number of scattering  $\text{P}_5\text{I}_5^+$  cations per volume). Therefore the intensity of the signals in the spectrum is low. For comparison: the 100% peak in the Raman spectrum of **3** spans only 0.1 Raman units while  $\text{P}_4$  and  $\text{PI}_3$  with the same conditions (laser power, sample sealed in NMR tube) have intensities of 3.0 to 5.0 Raman units for their 100% bands. This shows that already very small impurities of  $\text{P}_4$ ,  $\text{PI}_3$  or other intense Raman scatterers show in the obtained spectrum.
- Excess  $\text{P}_2\text{I}_4$  is insoluble at  $-90 \text{ }^\circ\text{C}$  and, therefore, invisible in the  $^{31}\text{P}$ -NMR at  $-90 \text{ }^\circ\text{C}$ .
- We could independently verify this assignment by directly synthesising and characterising  $\text{P}_2\text{I}_4[\text{Al}(\text{OR})_4]$ . We found that  $\text{P}_2\text{I}_5^+[\text{Al}(\text{OR})_4]^-$  is rapidly formed from 2  $\text{PI}_3$  and  $\text{Ag}(\text{CH}_2\text{Cl}_2)-[\text{Al}(\text{OR})_4]$ ; however, this is subject to ongoing research and will be published elsewhere.
- S. Pohl, *Z. Anorg. Allg. Chem.*, 1983, **498**, 20.
- C. Aubauer, G. Engelhardt, T. M. Klapötke and A. Schulz, *J. Chem. Soc., Dalton Trans.*, 1999, 1729.
- M. Hesse, H. Maier and B. Zeeh, *Spektroskopische Methoden in der Organischen Chemie*, 4th edn., 1991, Georg Thieme Verlag, Stuttgart–New York, p. 96.
- Although many crystals were tried and three full data sets were recorded at 170 K none of them gave a fully satisfactory result and the agreement factors were never better than 12.98%. However, the crystal system and space group are well determined and the thermal ellipsoids are normal. All trace electron density (about 1.0 to 1.3  $\text{e \AA}^{-3}$ ) appeared in the vicinity of the 18  $\text{CF}_3$  groups which suggested manifold rotational disorder as the reason for the bad agreement factors.
- The  $\text{Cl}_2\text{P}(\text{CHCl}_2)_2^+$  cation was fully optimised in  $\text{C}_2$  symmetry at the MP2/TZVPP level and all structural parameters of the cation in **1** could be reproduced in the gas phase within  $+0.02 \text{ \AA}$  and  $\pm 1^\circ$ , i.e.  $\text{P}-\text{Cl} = 1.953 \text{ \AA}$ ,  $\text{P}-\text{C} = 1.830 \text{ \AA}$ ,  $\text{C}-\text{Cl} = 1.751, 1.758 \text{ \AA}$ ,  $\text{Cl}-\text{P}-\text{Cl} = 110.9^\circ$ ,  $\text{C}-\text{P}-\text{C} = 110.4^\circ$ . For energies see ref. 26.
- For the geometry of  $\text{Cl}_2\text{P}(\text{CHCl}_2)_2^+$  see ref. 25; total energy:  $-3176.10253 \text{ a.u.}$ , ZPE: 0.04672,  $G$ :  $-0.00544$ .  $\text{CHCl}_3$  ( $\text{C}_{3v}$ ):  $d(\text{C}-\text{H}) = 1.087 \text{ \AA}$ ;  $d(\text{C}-\text{Cl}) = 1.763 \text{ \AA}$ , total energy:  $-1417.71307 \text{ a.u.}$ ; ZPE = 0.02027,  $G = -0.01092$ .
- S. Brownridge, H. D. B. Jenkins, I. Krossing, J. Passmore and H. K. Roobottom, *Coord. Chem. Rev.*, 2000, **197**, 397.
- J. A. Zimmerman, S. B. H. Bach, C. H. Watson and J. R. Eyler, *J. Chem. Phys.*, 1990, **95**, 98.
- It was shown convincingly that iodine substituents at tetra-coordinate phosphorus atoms lead to a very pronounced upfield shift due to relativistic spin–orbit coupling mediated to the nucleus by an effective Fermi contact mechanism.<sup>30</sup> Therefore only relativistic  $^{31}\text{P}$ -NMR shifts give meaningful answers as may be illustrated by the calculated non relativistic (NR) and relativistic (R) chemical shift of  $\text{PI}_4^+$ <sup>30</sup> which differ by over 700 ppm:  $\delta^{31}\text{P}_{\text{NR}} = +211$  and  $\delta^{31}\text{P}_{\text{NR}} = -520$ ! At present no routine for the standard calculation of relativistic NMR shifts is implemented in the current program codes.
- M. Kaupp, C. Aubauer, G. Engelhardt, T. M. Klapötke and O. Malkina, *J. Chem. Phys.*, 1999, **110**, 3897.
- A search of the chemical abstracts data base with Scifinder and the Cambridge structural database CSD with the program Conquest did not reveal a precedent for this  $\text{P}_5$ -cage. However, similar  $\text{C}_{2v}$  symmetric  $\text{MP}_4$  units (i.e.  $\text{M} = \text{Zr}, \text{Hf}$ ) formally containing a  $\text{P}_4^{2-}$  unit are known (see ref. 34).
- The chemical shifts of the naked or solvated  $\text{P}_5^+$  cation can be meaningfully computed since it bears no heavy iodine atoms.
- If not restrained by symmetry, the calculations always lead to  $\text{C}_{4v}$ - $\text{P}_5^+$ . Species containing  $\text{C}_{4v}$ - $\text{P}_5^+$  (and solvates) are true minima without imaginary frequencies and are lower in relative energy.
- O. J. Scherer, M. Swarowsky and G. Wolmershäuser, *Angew. Chem., Int. Ed. Engl.*, 1988, **27**, 694.
- I. Krossing, Habilitation thesis, University of Karlsruhe, 2002.
- C. Aubauer, M. Kaupp, T. M. Klapötke, H. Nöth, H. Pietrowski, W. Schnick and J. Senker, *J. Chem. Soc., Dalton Trans.*, 2001, 1880.
- J. E. Huheey, *Inorganic Chemistry*, 4th edn., Harper and Collins, New York, 1993.
- H. Schnöckel and S. Schunck, *Phosphorus, Sulfur, Silicon Relat. Elem.*, 1988, **39**, 89.
- Solvation energies were obtained from the MP2/TZVPP geometries using the COSMO model at the BP86/SVP level and dielectric constants for  $\text{CS}_2$  and  $\text{CH}_2\text{Cl}_2$  of 2.63 and 8.92 respectively.
- Thermal and entropic contributions to the enthalpy and free energy were obtained by fully optimising all the species in question with Gaussian98W at the semiempirical PM3 level. All these species also represented true minima without imaginary frequencies at the PM3 level. ZPE's were taken from the MP2 calculation. Since statistical

thermodynamics is only little influenced by the employed geometries and the entropic contributions mainly arise from the moment of inertia of a species, it is believed that errors associated with this procedure are very small if used consistently.

- 41 In agreement with this we succeeded in the preparation of  $P_5Br_2^+$  by reacting  $PBr_3$ ,  $P_4$  and  $Ag(CH_2Cl_2)[Al(OR)_4]$  in  $CH_2Cl_2$  (X-ray, Raman, NMR). However, this is subject to ongoing research and will be published elsewhere. A preliminary account appeared in *Angew. Chem.* (see ref. 10).
- 42 A. F. Holleman, E. Wiberg and N. Wiberg, *Lehrbuch der Anorganischen Chemie*, 101st edn., Walter de Gruyter, Berlin–New York, 1995, p. 1255.
- 43 D. Solan, *U. S. C. F. S. T. I. PB Rep.*, 1969, (PB-187819), p. 247; From *US Gov. Res. Dev. Rep.*, 1970, **70**, 61.
- 44 This U-shaped apparatus incorporates two bulbs stopped with J. Young valves. Both bulbs are connected by a glass tube including a fine sintered glass frit and the product side also included an additional valve that allowed the direct preparation of NMR samples of the reaction solution.
- 45 Gaussian 98, Revision A.3, Gaussian, Inc., Pittsburgh, PA, 1998.
- 46 TURBOMOLE, Version 5; (a) R. Ahlrichs, M. Bär, M. Häser, H. Horn and C. Kölmel, *Chem. Phys. Lett.*, 1989, **162**, 165; (b) M. v. Arnim and R. Ahlrichs, *J. Chem. Phys.*, 1999, **111**, 9183.
- 47 F. Weigend and M. Häser, *Theor. Chim. Acta*, 1997, **97**, 331.
- 48 (a) A. Schäfer, H. Horn and R. Ahlrichs, *J. Chem. Phys.*, 1992, **97**, 2571; (b) A. Schäfer, C. Huber and R. Ahlrichs, *J. Chem. Phys.*, 1994, **100**, 5829.
- 49 A. Klamt and G. Schürmann, *J. Chem. Soc., Perkin. Trans. 2*, 1993, 799.
- 50 G. M. Sheldrick, SHELX97, Program for crystal structure determination, University of Göttingen, Germany, 1997.